ANALYSES OF CAPSULE AN1-A
ARKANSAS POWER & LIGHT COMPANY
ARKANSAS NUCLEAR ONE, UNIT 1
-- Reactor Vessel Material Surveillance Program --

ANALYSES OF CAPSULE AN1-A
ARKANSAS POWER & LIGHT COMPANY
ARKANSAS NUCLEAR ONE, UNIT 1

-- Reactor Vessel Material Surveillance Program --

by

A. L. Lowe, Jr., PE
J. D. Aadland
L. L. Collins
L. A. Hassler
W. A. Pavinich
W. L. Redd

SUMMARY

This report describes the results of the examination of the third capsule of the Arkansas Power & Light Company's Arkansas Nuclear One, Unit 1 reactor vessel material surveillance program. The capsule was removed and examined after accumulating a fluence of 1.03×10^{19} n/cm^2 (E > 1 MeV), which is equivalent to approximately 30 effective full power years' operation of the reactor vessel. The objective of the program is to monitor the effects of neutron irradiation on the tensile and fracture toughness properties of the reactor vessel materials by the testing and evaluation of tension and Charpy impact specimens.

The capsule received an average fast fluence of 1.03×10^{19} n/cm^2 (E > 1.0 MeV) and the predicted fast fluence for the reactor vessel T/4 location at the end of the fifth cycle is 1.2×10^{18} n/cm^2 (E > 1 MeV). Based on the calculated fast flux at the vessel wall and an 80% load factor, the projected fast fluence that the Arkansas Nuclear One, Unit 1 reactor pressure vessel will receive in 40 calendar years' operation is 1.10×10^{19} n/cm^2 (E > 1 MeV).

The results of the tensile tests indicated that the materials exhibited normal behavior relative to neutron fluence exposure. The Charpy impact data results exhibited the characteristic behavior of shift to higher temperature for both the 30 and 50 ft-lb transition temperatures as a result of neutron fluence damage and a decrease in upper shelf energy. These results demonstrated that the current techniques used for predicting the change in both the increase in the RT_{NDT} and the decrease in upper shelf properties due to irradiation are conservative.

The recommended operating period was extended to 21 effective full power years as a result of this third capsule evaluation. These new operating limitations are in accordance with the requirements of Appendix G of 10 CFR 50.

CONTENTS

Babcock & Wilcox
a McDermott company

CONTENTS (Cont'd)

List of Tables

Babcock & Wilcox
a McDermott company

Tables (Cont'd)

List of Figures

Figures (Cont'd)

Babcock & Wilcox
a McDermott company

1. INTRODUCTION

This report describes the results of the examination of the third capsule of the Arkansas Power & Light Company's Arkansas Nuclear One, Unit 1 (ANO-1) reactor vessel material surveillance program (RVSP). The capsule was removed and examined after the equivalent of six years of operation of the ANO-1 reactor vessel. The capsule experienced a fluence of 1.03×10^{19} n/cm^2 (E > 1 MeV), which is the equivalent of approximately 30 effective full power years' (EFPY) operation of the reactor vessel. The first capsule from this program was removed and examined after the first year of operation; the results are reported in BAW-1440.[1] The second capsule was removed and examined after irradiation in Toledo Edison Company's Davis-Besse Unit 1 as part of the integrated reactor vessel materials surveillance program; the results are reported in BAW-1698.[2]

The objective of the program is to monitor the effects of neutron irradiation on the tensile and impact properties of reactor pressure vessel materials under actual operating conditions. The surveillance program for ANO-1 was designed and furnished by Babcock & Wilcox (B&W) as described in BAW-10006A.[3] The program was planned to monitor the effects of neutron irradiation on the reactor vessel materials for the 40-year design life of the reactor pressure vessel.

The surveillance program for ANO-1 was designed in accordance with E185-66 and thus is not in compliance with Appendixes G and H to 10 CFR 50 since the requirements did not exist at the time the program was designed. Because of this difference, additional tests and evaluations were required to ensure meeting the requirements of 10 CFR 50, Appendixes G and H. The recommendations for the future operation of ANO-1 included in this report do comply with these requirements.

Babcock & Wilcox
a McDermott company

2. BACKGROUND

The ability of the reactor pressure vessel to resist fracture is the primary factor in ensuring the safety of the primary system in light water-cooled reactors. The beltline region of the reactor vessel is the most critical region of the vessel because it is exposed to neutron irradiation. The general effects of fast neutron irradiation on the mechanical properties of such low-alloy ferritic steels as SA533, Grade B, and SA508, Cl. 2, used in the fabrication of the ANO-1 reactor vessel, are well characterized and documented in the literature. The low-alloy ferritic steels used in the beltline region of reactor vessels exhibit an increase in ultimate and yield strength properties with a corresponding decrease in ductility after irradiation. In reactor pressure vessel steels, the most serious mechanical property change is the increase in temperature for the transition from brittle to ductile fracture accompanied by a reduction in the upper shelf impact toughness.

Appendix G to 10 CFR 50, "Fracture Toughness Requirements," specifies minimum fracture toughness requirements for the ferritic materials of the pressure-retaining components of the reactor coolant pressure boundary (RCPB) of water-cooled power reactors, and provides specific guidelines for determining the pressure-temperature limitations on operation of the RCPB. The toughness and operational requirements are specified to provide adequate safety margins during any condition of normal operation, including anticipated operational occurrences and system hydrostatic tests, to which the pressure boundary may be subjected over its service lifetime. Although the requirements of Appendix G to 10 CFR 50 became effective on August 13, 1973, the requirements are applicable to all boiling and pressurized water-cooled nuclear power reactors, including those under construction or in operation on the effective date.

Appendix H to 10 CFR 50, "Reactor Vessel Materials Surveillance Program Requirements," defines the material surveillance program required to monitor

2-1

changes in the fracture toughness properties of ferritic materials in the reactor vessel beltline region of water-cooled reactors resulting from exposure to neutron irradiation and the thermal environment. Fracture toughness test data are obtained from material specimens withdrawn periodically from the reactor vessel. These data will permit determination of the conditions under which the vessel can be operated with adequate safety margins against fracture throughout its service life.

A method for guarding against brittle fracture in reactor pressure vessels is described in Appendix G to the American Society of Mechanical Engineers (ASME) Boiler and Pressure Vessel Code, Section III, "Nuclear Power Plant Components." This method utilizes fracture mechanics concepts and the reference nil-ductility temperature, RT_{NDT}, which is defined as the greater of the drop weight nil-ductility transition temperature [according to the American Society for Testing and Materials (ASTM) Standard E208] or the temperature that is 60F below that at which the material exhibits 50 ft-lbs and 35 mils lateral expansion (MLE). The RT_{NDT} of a given material is used to index that material to a reference stress intensity factor curve (K_{IR} curve), which appears in Appendix G of ASME Section III. The K_{IR} curve is a lower bound of dynamic, static, and crack arrest fracture toughness results obtained from several heats of pressure vessel steel. When a given material is indexed to the K_{IR} curve, allowable stress intensity factors can be obtained for this material as a function of temperature. Allowable operating limits can then be determined using these allowable stress intensity factors.

The RT_{NDT} and, in turn, the operating limits of a nuclear power plant, can be adjusted to account for the effects of radiation on the properties of the reactor vessel materials. The radiation embrittlement and the resultant changes in mechanical properties of a given pressure vessel steel can be monitored by a surveillance program in which a surveillance capsule containing prepared specimens of the reactor vessel materials is periodically removed from the operating nuclear reactor and the specimens are tested. The increase in the Charpy V-notch 30 ft-lb temperature is added to the original RT_{NDT} to adjust it for radiation embrittlement. This adjusted RT_{NDT} is used to index the material to the K_{IR} curve which, in turn, is used to set operating limits for the nuclear power plant. These new limits take into account the effects of irradiation on the reactor vessel materials.

2-2

Babcock & Wilcox
a McDermott company

3. SURVEILLANCE PROGRAM DESCRIPTION

The surveillance program for ANO-1 comprises six surveillance capsules designed to allow the owner to monitor the effects of the neutron and thermal environment on the materials of the reactor pressure vessel core region. The capsules, which were inserted into the reactor vessel before initial plant startup, were positioned inside the vessel between the thermal shield and the vessel wall at the locations shown in Figure 3-1. The six capsules, placed two in each holder tube, were positioned near the peak axial and azimuthal neutron flux. BAW-10006A includes a full description of the capsule locations and design.[3] After the capsules were removed from ANO-1 and included in the integrated RVSP, they were scheduled for irradiation in the Davis-Besse Unit 1 reactor as described in BAW-1543.[4] During this period of irradiation, capsule AN1-A was irradiated in site YZ as shown in Figure 3-2.

Capsule AN1-A was removed from Davis-Besse Unit 1 after cycle 3 and an accumulated fluence of approximately 1.0×10^{19} n/cm^2 (E > 1 MeV). This capsule contained Charpy V-notch impact and tensile specimens fabricated of SA533, Grade B Class 1 base metal, weld metal, Charpy V-notch impact specimens of heat-affected zone (HAZ) material and the correlation monitor material.* The specimens contained in the capsule are described in Table 3-1 and shown in Figure 3-3, and the chemistry and heat treatment of the surveillance material in capsule AN1-A are described in Table 3-2. The chemistry and heat treatment of the correlation material are presented in Table 3-3.

All test specimens were machined from the 1/4-thickness (1/4T) location of the plates. Charpy V-notch and tensile specimens from the vessel material were oriented with their longitudinal axes parallel to the principal rolling direction of the plate; Charpy V-notch specimens were also oriented

- - - - -
*The correlation monitor material is from the Heavy Section Steel Technology (HSST) Program.

Babcock & Wilcox
a McDermott company

transverse to the principal rolling direction. Weld metal specimens were oriented to measure the properties of the weld metal; the tensile specimens were oriented with their longitudinal axis parallel to the weld groove (all weld metal tensile specimens), while Charpy specimens were oriented with their notches oriented in the center of the weld in the longitudinal direction. The HAZ Charpy V-notch specimens were oriented with their longitudinal axes transverse to the weld groove, with the notch in the base metal, and directed parallel to the axis of the weld.

Capsule AN1-A contained the following types of dosimeter wires:

Dosimeter wire	Shielding
U-Al alloy	Cd-Ag alloy
Np-Al alloy	Cd-Ag alloy
Nickel	Cd-Ag alloy
0.66 wt % Co-Al alloy	Cd-Ag alloy
0.66 wt % Co-Al alloy	None
Fe	None

Thermal monitors of low-melting eutectic alloys and pure metal were included in the capsule. The monitors and their melting points are as follows:

Alloy	Melting point, F
90% Pb, 5% Ag, 5% Sn	558
97.5% Pb, 2.5% Ag	580
97.5% Pb, 1.5% Ag, 1.0% Sn	588
Cadmium	610
Lead	621

Babcock & Wilcox
a McDermott company

Table 3-1. Specimens in Surveillance Capsule AN1-A

| | Number of test specimens | |
Material description	Tension	CVN[a] impact
Weld metal, WF 193	4	8
HAZ		
Heat No. C5114-1, longitudinal	0	8
Base material plate		
Heat No. C5114-1, longitudinal	4	8
transverse	0	4
Correlation, HSST plate 02	0	8
Total per capsule	8	36

[a]CVN denotes Charpy V-notch.

Babcock & Wilcox
a McDermott company

Table 3-2. Chemistry and Heat Treatment of
Surveillance Materials

Chemical Analysis

Element	Heat No.[a] C5114-1	Weld metal WF 193[b]	Weld metal WF 193[c]
C	0.21	0.065	0.09
Mn	1.32	1.50	1.49
P	0.010	0.016	0.016
S	0.016	0.008	0.016
Si	0.20	0.42	0.51
Ni	0.52	0.59	0.59
Cr	--	--	0.06
Mo	0.57	0.36	0.39
Cu	0.15	0.19	0.28

Heat Treatment

Heat No.	Temp, F	Time, h	Cooling
C5114-1[a]	1550-1600	4.5	Brine-quenched
	1200-1225	5.0	Brine-quenched
	1100-1150	40.0	Furnace-cooled
WF 193	1100-1150	29	Furnace-cooled

[a]Per Certified Materials Test Report.

[b]Per Weld Procedure Qualification Test Record.

[c]Per Licensing Document BAW-1500.

Babcock & Wilcox
a McDermott company

Table 3-3. Chemistry and Heat Treatment of Correlation
Material -- Heat A-1195-1, A533 Grade B,
Class 1 (HSST Plate 02)

Chemical Analysis (1/4T)[a]

Element	wt %
C	0.23
Mn	1.39
P	0.013
S	0.013
Si	0.21
Ni	0.64
Mo	0.50
Cu	0.17

Heat Treatment[b]

1. Normalized at 1675F ± 75F.
2. 1600F ± 75F for 4 h/water-quenched.
3. 1225F ± 25F for 4 h/furnace-cooled.
4. 1125F ± 25F for 40 h/furnace-cooled.

[a]ORNL-4463.

[b]Per identification card; heat treatment
by Combustion Engineering.

Babcock & Wilcox
a McDermott company

Figure 3-1. Reactor Vessel Cross Section Showing Surveillance
Capsule Locations at ANO-1

Babcock & Wilcox
a McDermott company
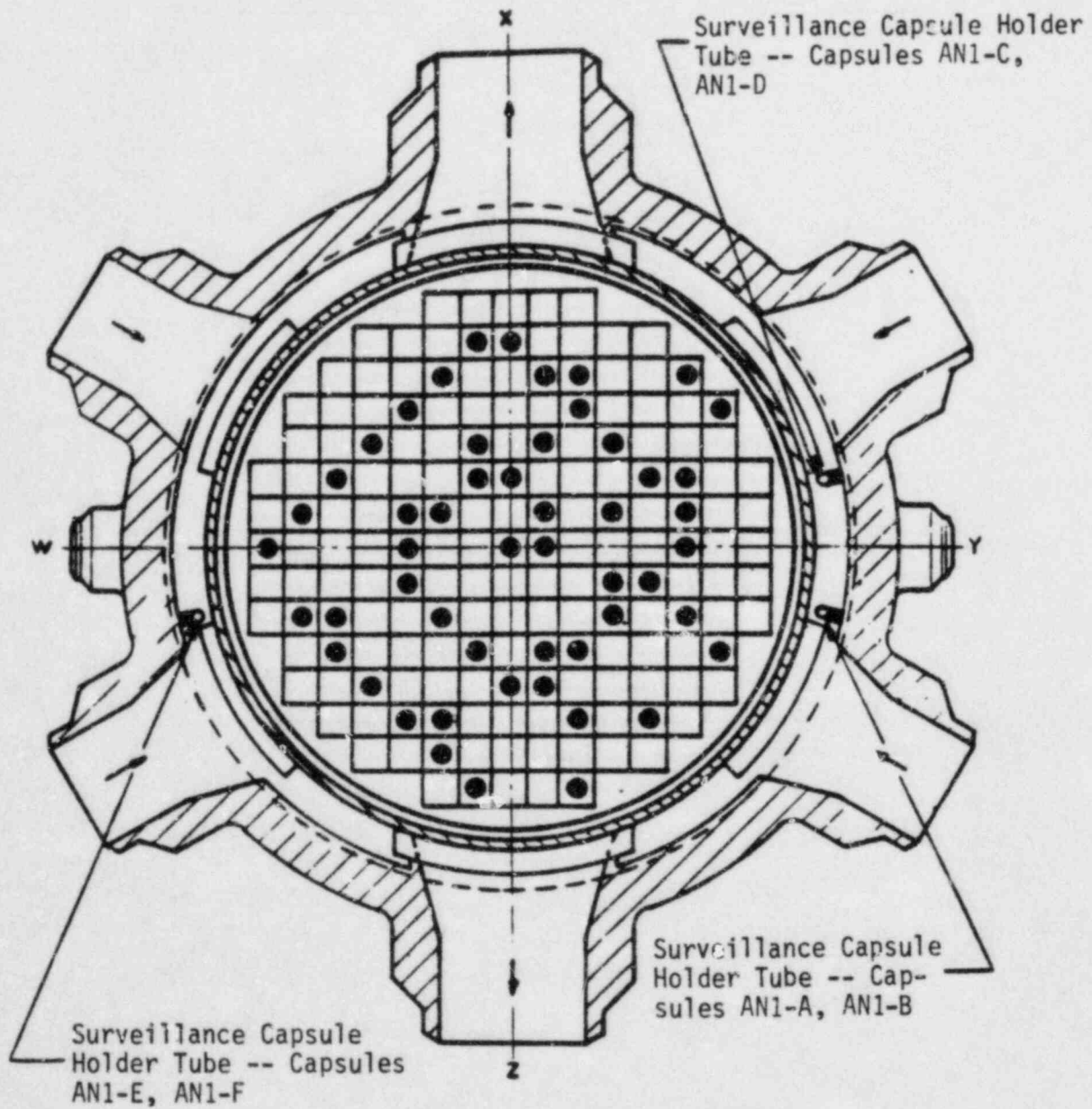
Figure 3-2. Reactor Vessel Cross Section Showing Location of
ANO-1 Capsule in Davis-Besse Unit 1 Reactor

Babcock & Wilcox
a McDermott company
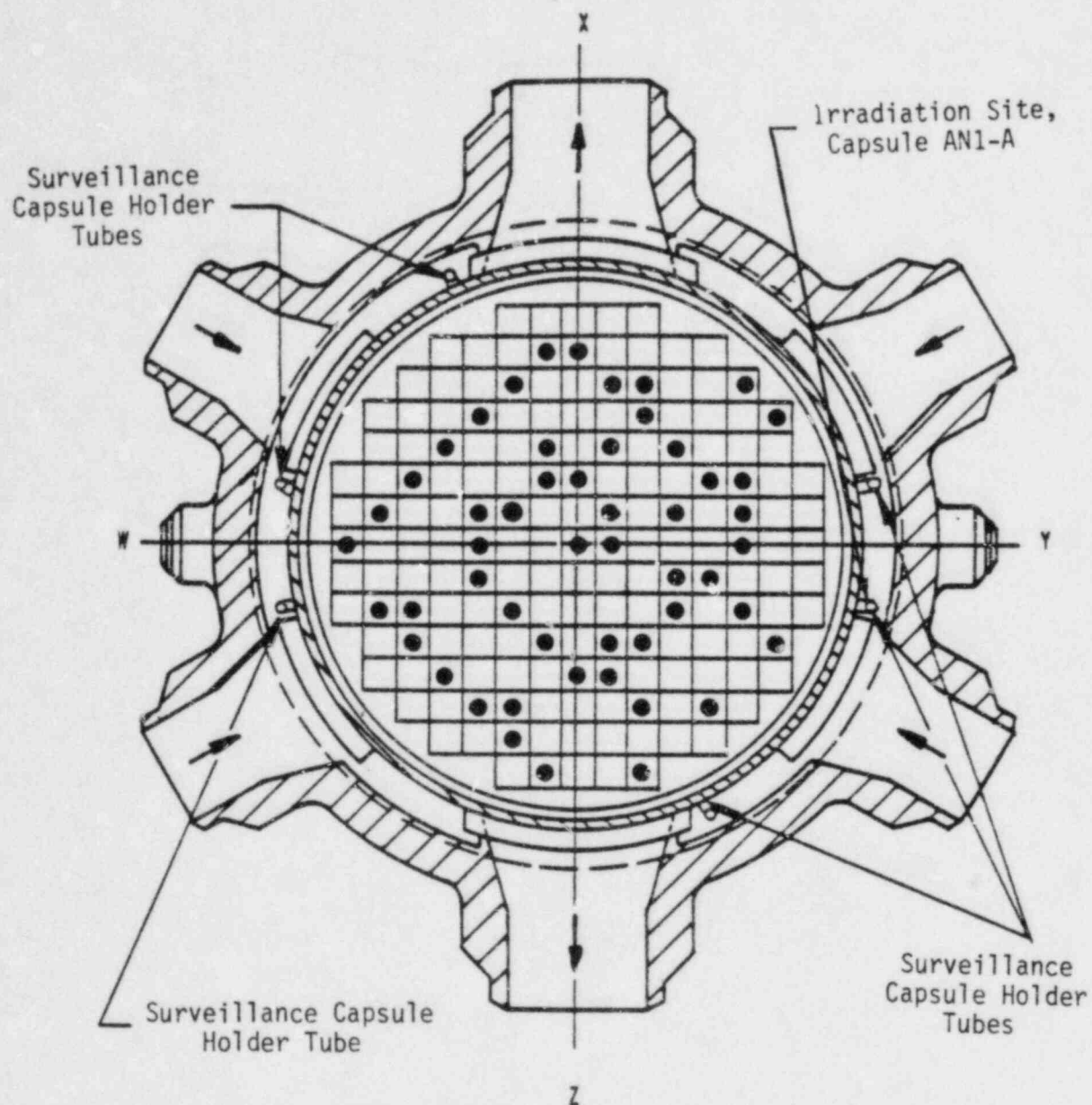
Tension Test Specimens
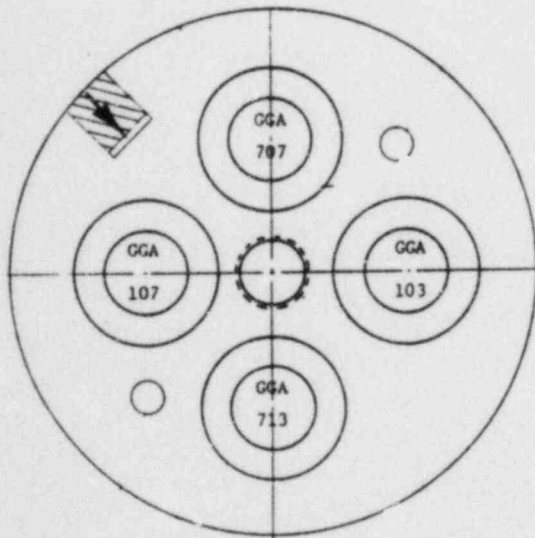
STACK
FROM
TOP

First   Second
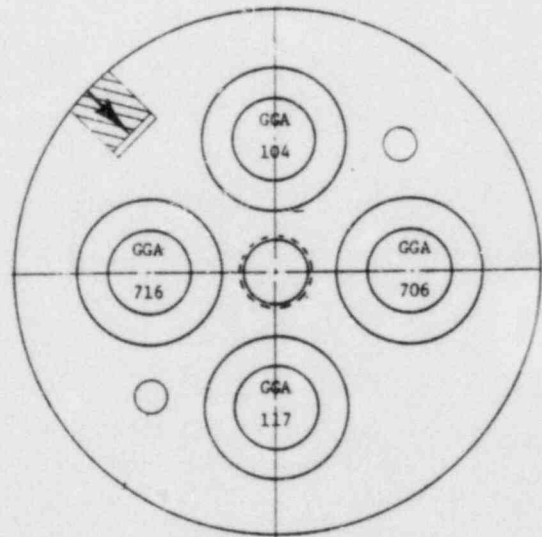
Note: Arrow indicates position of orientation key.

Figure 3-3. Loading Diagram for Test
Specimens in AN1-A

Charpy Specimens

GGA	GGA
414	604
GGA	GGA
60?	443
GGA	GGA
709	439

GGA	GGA	GGA
421	939	037
GGA	GGA	GGA
702	010	935
GGA	GGA	GGA
008	436	40?

GGA	GGA	GGA
932	710	720
GGA	GGA	GGA
040	940	617
GGA	GGA	GGA
904	619	015

GGA	GGA	GGA
026	942	033
GGA	GGA	GGA
918	949	713
GGA	GGA	GGA
401	003	701

Third   Fourth   Fifth   Sixth

TI
**APERTURE
CARD**

Also Available On
Aperture Card

8408140433-01

Babcock & Wilcox
a McDermott company

4. PREIRRADIATION TESTS

Unirradiated material was evaluated for two purposes: (1) to establish a baseline of data to which irradiated properties data could be referenced, and (2) to determine those materials properties to the extent practical from available material, as required for compliance with Appendixes G and H to 10 CFR 50.

4.1. Tensile Tests

Tensile specimens were fabricated from the reactor vessel shell course plate and weld metal. The small-size specimens were 4.25 inches long with a reduced section 1.750 inches long by 0.357 inch in diameter. They were tested on a 20,000-lb load capacity universal test machine at a crosshead speed of 0.005 inch per minute. A linear voltage differential transformer (LVDT) type clamp-end screw-on extensometer was used to determine the 0.2% yield point. Test conditions were in accordance with the applicable requirements of ASTM A370-72. For each material type and/or condition, six specimens in groups of three were tested at both room temperature and 570F. The tension-compression load cell used had a certified accuracy of better than ±0.5% of full scale (10,000 lb). All test data for the preirradiation tensile specimens are given in Appendix B.

4.2. Impact Tests

Charpy V-notch impact tests were conducted in accordance with the requirements of ASTM Standard Methods A370-72 and E23-72 on an impact tester certified to meet Watertown standards. Test specimens were of the Charpy V-notch type, which were 0.394 inch square and 2.165 inches long.

Before testing, specimens were temperature-conditioned in a combination resistance-heated/carbon dioxide-cooled chamber, designed to cover the temperature range from -85 to +550F. The specimen support arm, which was linked to the pneumatic transfer mechanism, is instrumented with a contacting

thermocouple allowing instantaneous specimen temperature determinations. Specimens were transferred from the conditioning chamber to the test frame anvil and precisely pretest-positioned with a fully automated, remotely controlled apparatus. Transfer times were less than 3 seconds and repeat within 0.1 second. Once the specimen was positioned, the electronic interlock opened, and the pendulum was released from its preset drop height. After failing the specimen, the hammer pendulum was slowed on its return stroke and raised back to its start position.

Impact test data for the unirradiated baseline reference materials are presented in Appendix C. Tables C-1 through C-4 contain the basis data that are plotted in Figures C-1 through C-4.

Babcock & Wilcox
a McDermott company

5. POSTIRRADIATION TESTS

5.1. Thermal Monitors

Capsule AN1-A contained three temperature monitor holder tubes, each containing five fusible alloy wires with melting points ranging from 558 to 621F. All the thermal monitors at 558, 580, and 588F had melted, while those at the 610F location showed partial melting or slumping; the monitor at the 621F location melted in all three holder tubes. It is therefore assumed that the 610 and 621F monitors were placed in the wrong locations in the holder tubes. From these observations, it was concluded that the capsule had been exposed to a peak temperature in the range of 610 to 621F during the reactor operating period. These peak temperatures are attributed to operating transients that are of short durations and are judged to have an insignificant effect on irradiation damage. Short duration operating transients cause the use of thermal monitor wires to be of limited value in determining the maximum steady-state operating temperature of the surveillance capsules; however, it is judged that the maximum steady-state operating temperature of specimens in the capsule was held within ±25F of tne 1/4T vessel thickness location temperature of 577F.[*] It is concluded that the capsule design temperature may have been exceeded during operating transients but not for times and temperatures that would preclude the use of the capsule data.

5.2. Tensile Test Results

The results of the postirradiation tensile tests are presented in Table 5-1. Tests were performed on specimens at room temperature, 580F, and two intermediate temperatures. The specimens were tested on a 55,000-lb load capacity universal test machine at a crosshead speed of 0.005 inch per

- - - - -

[*]G. A. Wickstrom, "Thermal Analysis of Redesigned 177-FA SSHT," Babcock & Wilcox Document <u>32-3728-00</u>, May 28, 1976.

Babcock & Wilcox
a McDermott company

minute up to yielding, and 0.050 inch per minute thereafter. A four-pole extension device with a strain-gaged extensometer was used to determine the 0.2% yield point. Test conditions were in accordance with the applicable requirements of ASTM A370-77. The tension-compression load cell used had a certified accuracy of better than ±0.5% of full scale (25,000 lb). In general, the ultimate strength and yield strength of the material increased with a corresponding decrease in ductility; both effects were the result of neutron radiation damage. The type of behavior observed and the degree to which the material properties changed is within the range of changes to be expected for the radiation environment to which the specimens were exposed.

5.3. Charpy V-Notch Impact Test Results

The test results from the irradiated Charpy V-notch specimens of the reactor vessel beltline material and the correlation monitor material are presented in Tables 5-2 through 5-6 and Figures 5-1 through 5-5. The tests were conducted in accordance with the requirements of ASTM Standard Methods A370-77 and E23-82 on an impact tester certified to meet Watertown standards. Test specimens were of the Charpy V-notch type, which were 0.394 inch square and 2.165 inches long. Prior to testing, specimens were temperature-controlled in liquid immersion baths capable of covering the temperature range from -85 to +550F. Specimens were removed from the baths and positioned in the test frame anvil with tongs specifically designed for the purpose. The pendulum was released manually, allowing the specimens to be broken within 5 seconds from their removal from the temperature baths. The data show that the material exhibited a sensitivity to irradiation within the values predicted from its chemical composition and the fluence to which it was exposed.

Table 5-1. Tensile Properties of Capsule AN1-A Base Metal and
Weld Metal Irradiated to 1.03E19 n/cm² (E > 1 MeV)

Specimen No.	Test temp, F	Strength, psi		Elongation, %		Red'n in area, %
		Yield	Ultimate	Unif.	Total	
Base Metal, Longitudinal						
GG 713	76	78,700	99,700	11	24	55
GG 706	300	71,900	93,500	10	22	64
GG 716	400	70,100	92,200	10	22	64
GG 707	580	69,700	94,800	11	23	61
Weld Metal						
GG 107	76	84,100	99,200	12	24	54
GG 117	285	77,400	92,800	10	20	48
GG 104	400	76,100	90,800	10	20	53
GG 103	580	73,200	91,600	10	19	47

Table 5-2. Charpy Impact Data From Capsule AN1-A, HAZ
Metal, Longitudinal Orientation, Irradiated
to 1.03E19 n/cm² (E > 1 MeV)

Specimen No.	Test temp, F	Absorbed energy, ft-lb	Lateral expansion, 10^{-3} in.	Shear fracture, %
GG 421	-63	19.0	16	5
GG 414	-2	30.0	17	20
GG 436	32	38.0	26	30
GG 443	75	44.0	40	50
GG 401	153	66.0	47	100
GG 432	222	72.0	60	100
GG 405	378	74.0	52	100
GG 439	454	69.0	73	100

Babcock & Wilcox
a McDermott company

Table 5-3. Charpy Impact Data From Capsule AN1-A, Base Metal, Transverse Orientation, Irradiated to 1.03E19 n/cm^2 (E > 1 MeV)

Specimen No.	Test temp, F	Absorbed energy, ft-lb	Lateral expansion, 10^{-3} in.	Shear fracture, %
GG 617	0	10.0	8	0
GG 601	75	33.0	29	10
GG 619	153	46.0	38	10
GG 604	222	83.0	77	100
GG 627	441	78.0	67	100

Table 5-4. Charpy Impact Data From Capsule AN1-A, Base Metal, Longitudinal Orientation, Irradiated to 1.03E19 n/cm^2 (E > 1 MeV)

Specimen No.	Test temp, F	Absorbed energy, ft-lb	Lateral expansion, 10^{-3} in.	Shear fracture, %
GG 713	-2	22.0	17	0
GG 723	32	35.0	30	5
GG 709	75	52.0	37	30
GG 710	115	57.0	47	45
GG 720	153	99.0	72	100
GG 702	268	108.0	80	100
GG 701	378	104.0	91	100

Table 5-5. Charpy Impact Data From Capsule AN1-A, Weld Metal
WF 193 Irradiated to $1.03E19$ n/cm^2 (E > 1 MeV)

Specimen No.	Test temp, F	Absorbed energy, ft-lb	Lateral expansion, 10^{-3} in.	Shear fracture, %
GG 026	75	12.0	12	0
GG 040	115	22.0	22	10
GG 010	153	28.0	24	20
GG 008	222	43.0	41	100
GG 033	268	42.0	53	100
GG 003	326	47.0	47	100
GG 015	378	43.0	42	100
GG 037	454	45.0	47	100

Table 5-6. Charpy Impact Data From Capsule AN1-A, Correlation
Monitor Material, Heat No. A-1195-1, Longitudinal
Orientation, Irradiated to $1.03E19$ n/cm^2 (E > 1 MeV)

Specimen No.	Test temp, F	Absorbed energy, ft-lb	Lateral expansion, 10^{-3} in.	Shear fracture, %
GG 940	32	10.0	9	0
GG 939	75	23.0	20	5
GG 942	156	32.0	30	15
GG 918	192	72.0	56	80
GG 932	222	75.0	55	95
GG 904	302	87.0	78	100
GG 935	378	96.0	75	100
GG 949	454	94.0	73	100

Babcock & Wilcox
a McDermott company

Figure 5-1. Charpy Impact Data for Shell Plate Material, HAZ, Longitudinal Orientation

DATA SUMMARY

T_{NDT}	--
T_{CV} (35 MLE)	60F
T_{CV} (50 FT-LB)	90F
T_{CV} (30 FT-LB)	2F
C_V-USE (AVG)	74 ft-lbs
RT_{NDT}	--

MATERIAL SA533, Gr B
ORIENTATION HAZ -- Long.
FLUENCE 1.03E19 n/cm^2
HEAT No. C 5114-1

454F

Babcock & Wilcox
a McDermott company
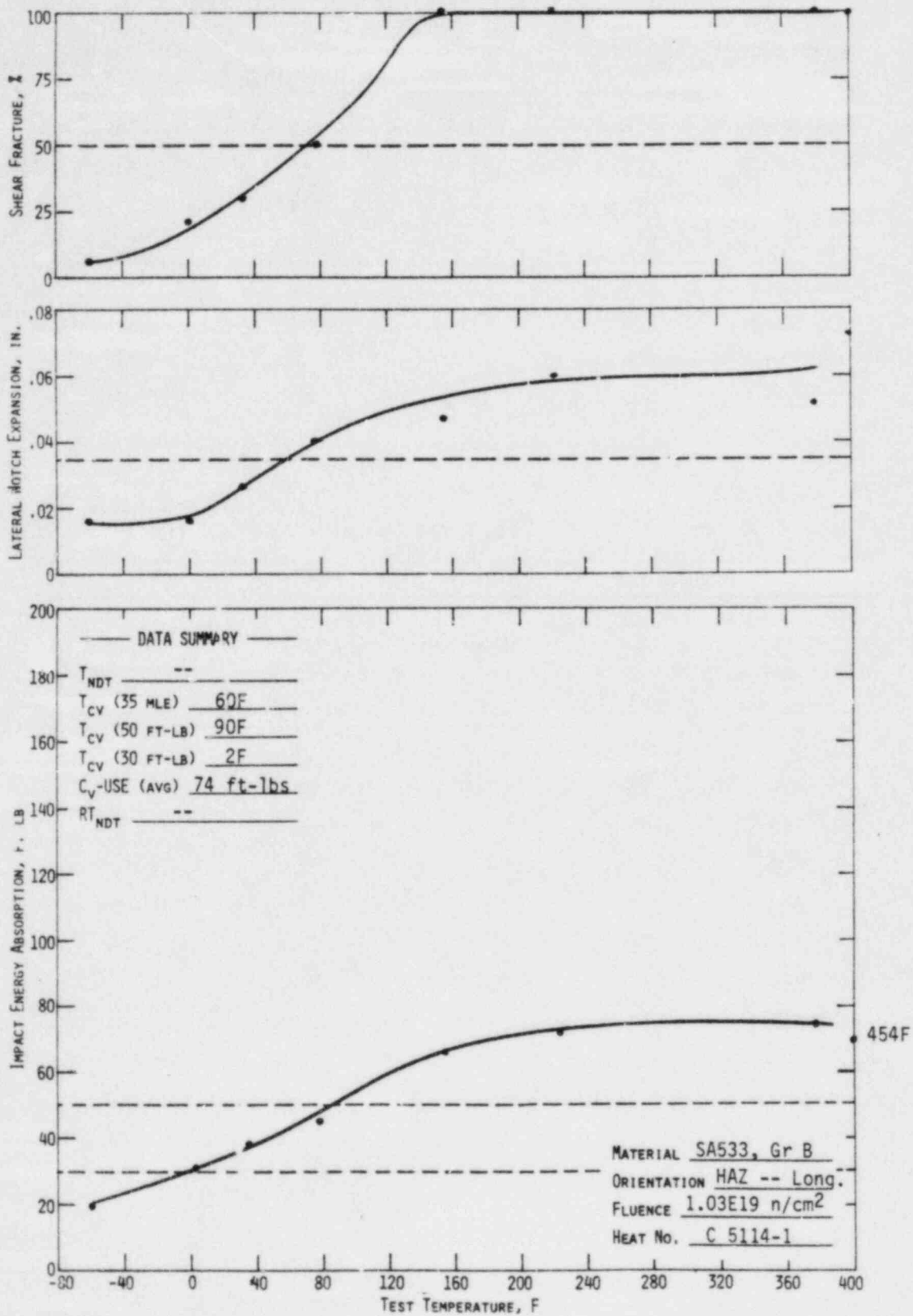
Figure 5-2. Charpy Impact Data for Shell Plate Material,
Transverse Orientation

Data Summary:

T_{NDT}	--
T_{CV} (35 MLE)	127F
T_{CV} (50 FT-LB)	144F
T_{CV} (30 FT-LB)	83F
C_V-USE (AVG)	83 ft-lbs
RT_{NDT}	--

MATERIAL	SA533, Gr B
ORIENTATION	Transverse
FLUENCE	1.03E19 n/cm^2
HEAT No.	C 5114-1

Babcock & Wilcox
a McDermott company
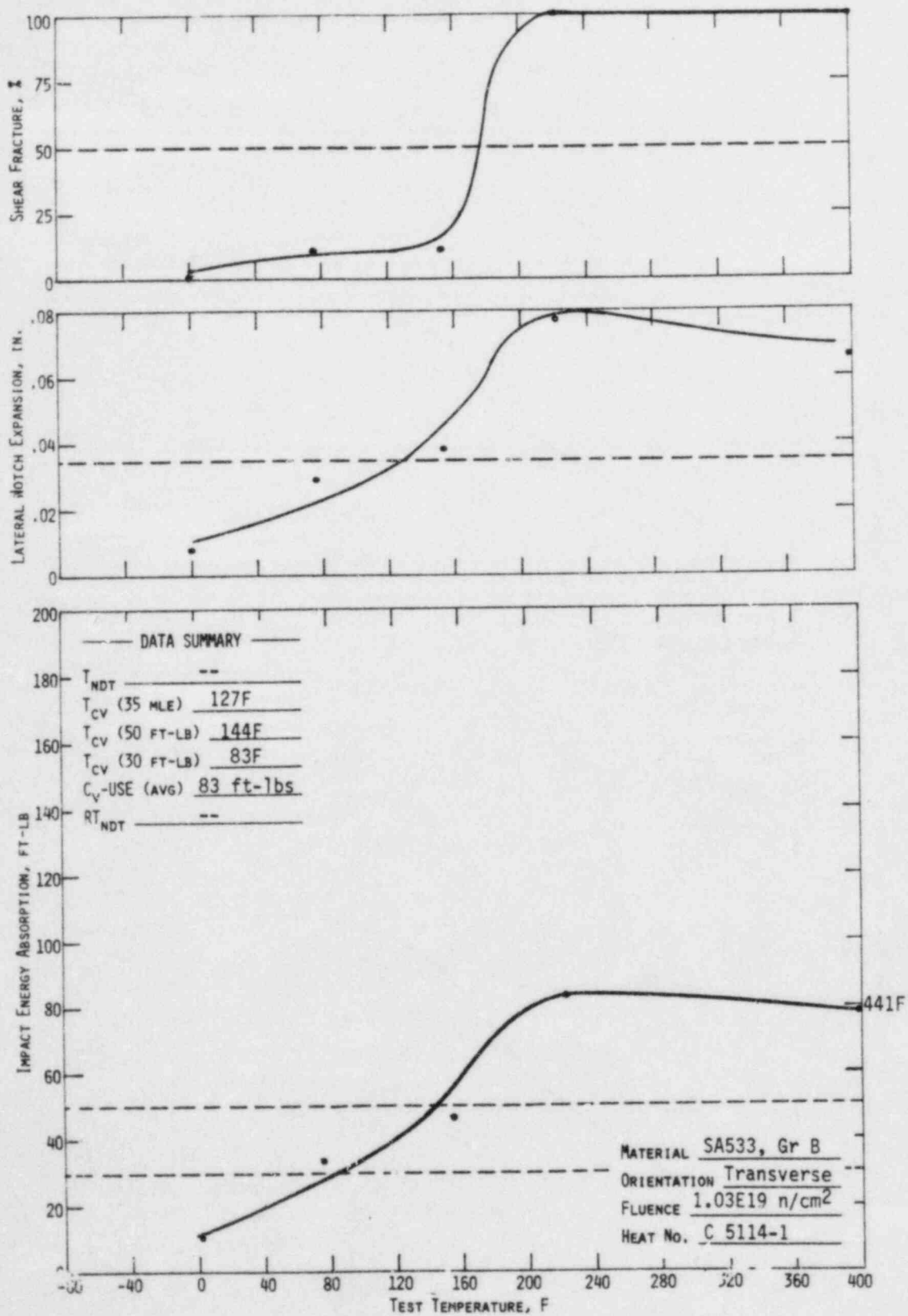
Figure 5-3. Charpy Impact Data for Shell Plate Material,
Longitudinal Orientation

Babcock & Wilcox
a McDermott company
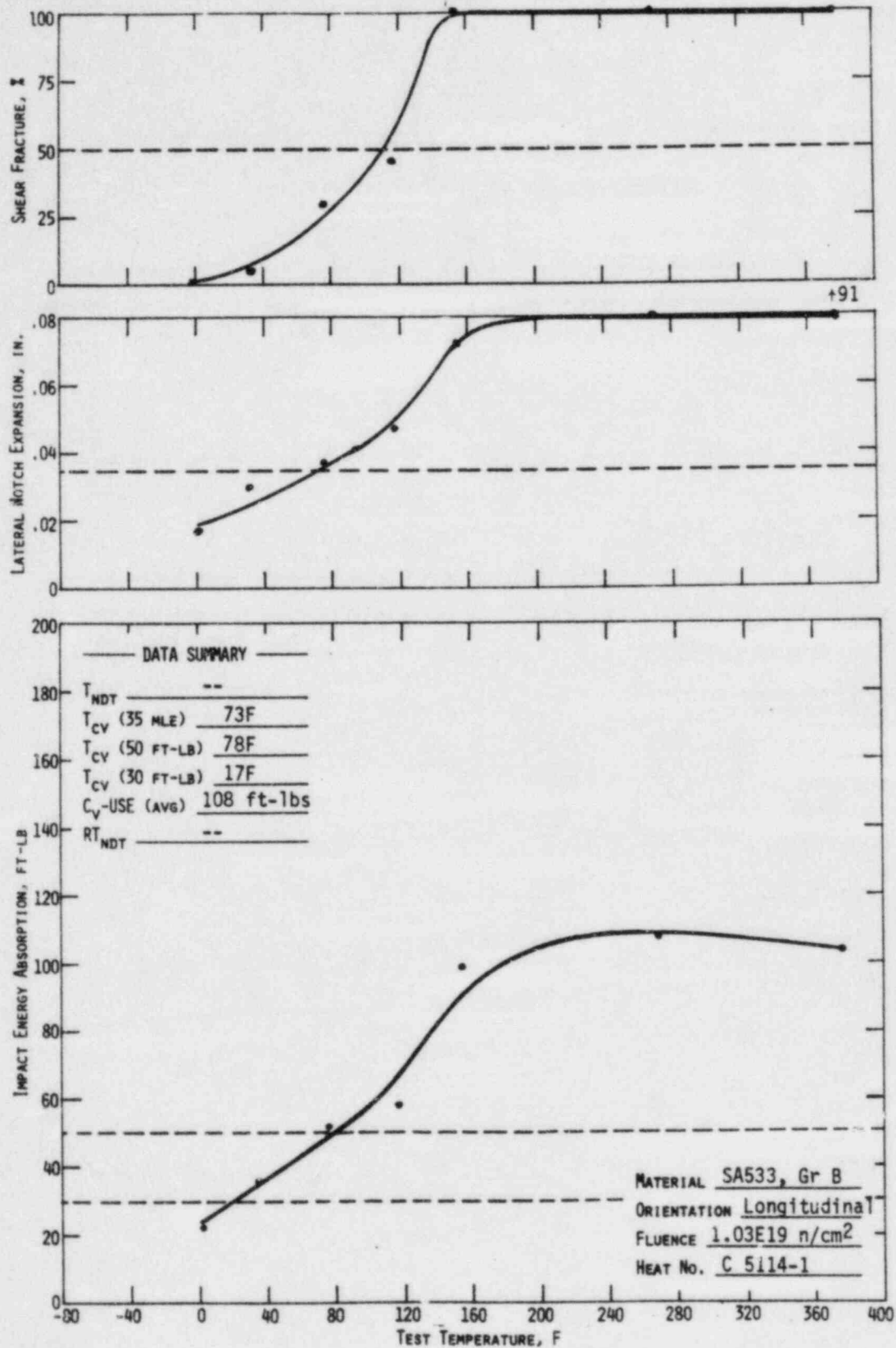
Figure 5-4. Charpy Impact Data for Weld Metal WF 193

DATA SUMMARY

T_{NDT} --
T_{CV} (35 MLE) 194F
T_{CV} (50 FT-LB) N.D.
T_{CV} (30 FT-LB) 156F
C_V-USE (AVG) 45 ft-lbs
RT_{NDT} --

MATERIAL Weld Metal
ORIENTATION
FLUENCE 1.03E19 n/cm^2
HEAT No. WF 193

Babcock & Wilcox
a McDermott company
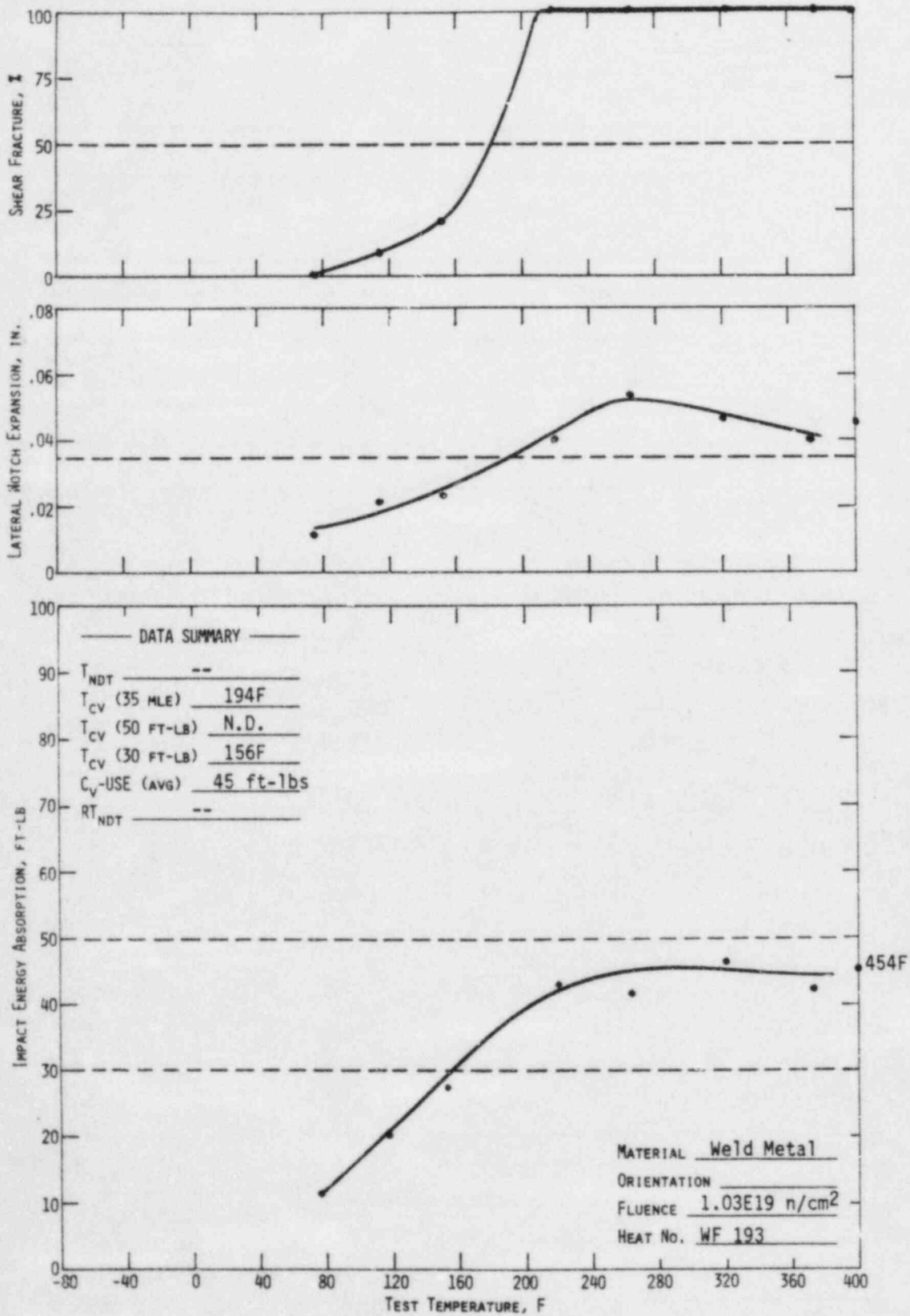
Figure 5-5. Charpy Impact Data for Correlation Monitor Material,
HSST Plate 02, Heat No. A-1195-1

DATA SUMMARY

T_{NDT} ----
T_{CV} (35 MLE)   140F
T_{CV} (50 FT-LB) 140F
T_{CV} (30 FT-LB)   94F
C_V-USE (AVG)   95 ft-lbs
RT_{NDT} ----

MATERIAL HSST Plate 02
ORIENTATION Longitudinal
FLUENCE 1.03E19 n/cm^2
HEAT No. A-1195-1

Babcock & Wilcox
a McDermott company
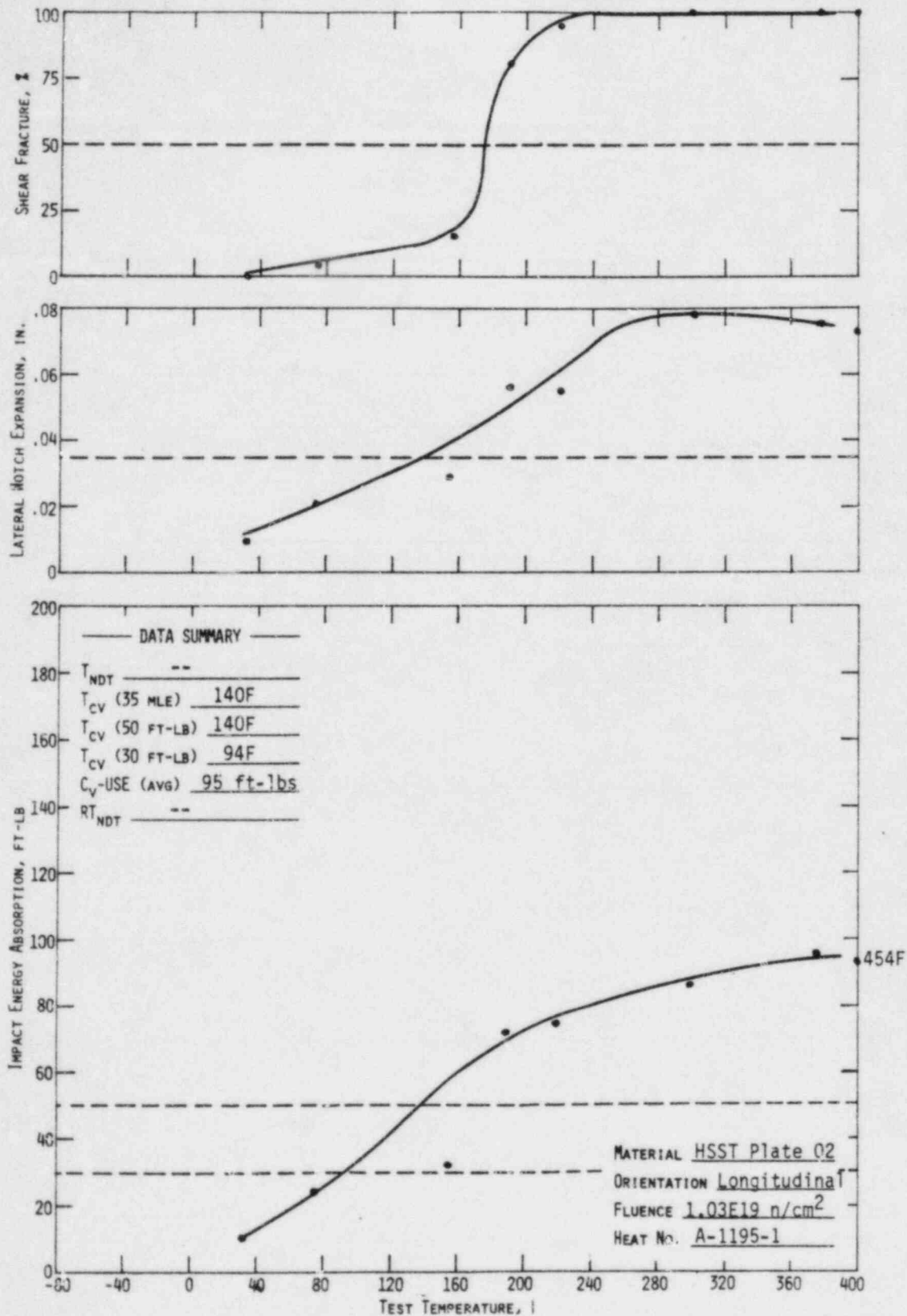
6. NEUTRON DOSIMETRY

6.1. Background

Fluence analysis as a part of the reactor vessel surveillance program has three objectives: (1) determination of maximum fluence at the pressure vessel as a function of reactor operation, (2) prediction of pressure vessel fluence in the future, and (3) determination of the test specimen fluence within the surveillance capsule. Vessel fluence data are used to evaluate changes in the reference transition temperature and upper shelf energy levels, and to establish a correlation between changes in material properties and fluence exposure. Fluence data are obtained either directly or indirectly from flux distributions calculated with a computer model of the reactor. The accuracy of calculated fast flux is enhanced by the use of a normalization factor that utilizes measured activity data obtained from capsule dosimeters.

A significant aspect of the surveillance program is to provide a correlation between the neutron fluence above 1 MeV and the radiation-induced property changes noted in the surveillance specimens. To permit such a correlation, activation detectors with reaction thresholds in the energy range of interest were placed in each surveillance capsule. The significant properties of the detectors are given in Tables 6-1 and E-1.

Because of a long half-life (30 years) and effective threshold energies of 0.5 and 1.1 MeV, the measurements of ^{137}Cs production from fission reactions in ^{237}Np and ^{238}U are more directly applicable to analytical determinations of the fast neutron fluence (E > 1 MeV) for multiple fuel cycles than are other dosimeter reactions. Other dosimeter reactions are useful as corroborating data for shorter time intervals and/or higher energy fluxes. Short-lived isotope activities are representative of reactor conditions only over the latter portion of the irradiation period (fuel cycle), whereas reactions with a threshold energy greater than 2 or 3 MeV do not record a significant part of the total fast flux.

Babcock & Wilcox
a McDermott company

The energy-dependent neutron flux is not directly available for activation detectors because the dosimeters register only the integrated effect of neutron flux on the target material as a function of both irradiation time and neutron energy. To obtain an accurate estimate of the average neutron flux incident upon the detector, several parameters must be known: the operating history of the reactor, the energy response of the given detector, and the neutron spectrum at the detector location. Of these parameters, the definition of the neutron spectrum is the most difficult to obtain. Essentially two means are available to obtain the spectrum: iterative unfolding of experimental dosimeter data and/or analytical methods. Because of a lack of sufficient threshold reaction detectors satisfying both the threshold energy and half-life requirements of a surveillance program, calculated spectra have been used.

Neutron transport calculations in two-dimensional geometry are used to obtain energy-dependent flux distributions throughout the reactor system. Reactor conditions are selected to be representative of an average over the irradiation time period. Geometric detail is selected to explicitly represent the reactor system to provide the flux distributions in the reactor vessel. The capsule flux distributions were obtained in previous analyses which modeled an explicit surveillance capsule assembly. The capsule energy-dependent flux distribution enabled the generation of calculated dosimeter activities. A comparison of the measured to calculated activities provided the normalization factor applied to the calculated vessel flux and fluence. Due to consistency in both the normalization factors and calculated average reaction cross sections from the previous analyses, the explicit calculation of capsule flux was not used in this analysis; rather an average capsule flux was obtained directly from the measured data using the average cross sections. In addition, the average normalization factor from previous analyses was applied to the vessel flux to normalize it to measured values. Use of this method has provided results that are consistent with previously reported results. A more detailed description of this revised calculational procedure is contained in Appendix D.

6.2. Vessel Fluence

The maximum fluence ($E > 1.0$ MeV) in the pressure vessel during ANO-1 cycle 5 was determined to be 3.96 (+17) n/cm^2 based on a maximum neutron flux of

Babcock & Wilcox
a McDermott company

1.03 (+10) n/cm^2-s (Tables 6-2 and 6-3). The location of maximum fluence is a point at the cladding/vessel interface at an elevation of about 103 cm above the lower active fuel boundary and at an azimuthal (peripheral) location of about 8 degrees from a major axis (across flats diameter). Fluence data have been extrapolated to 32 EFPY of operation based on the premise that excore flux is proportional to fast flux escaping the core (Appendix D). Core escape flux values are available from fuel management analyses of the current and future fuel cycles that have been designed. For ANO-1, future cycles 6 and 7 are available, and cycle 7 has been assumed to be the equilibrium cycle used for extrapolation to 32 EFPY.

Relative fluence as a function of radial location in the reactor vessel is shown in Figure 6-1. Reactor vessel lead factors (clad interface flux/in-vessel flux) for the T/4, T/2, 3T/4 locations are 1.8, 3.6, and 7.7, respectively. Relative fluence as a function of azimuthal angle for cycle 5 is shown in Figure 6-2. A peak occurs at about 8 degrees which roughly corresponds to a radius through a corner of the core and the position of the surveillance holder tube. The ratio of fast flux at the maximum and minimum locations is about 1.5. Previous analyses have shown this peak to be about 10 degrees with all fresh fuel in the flats assemblies. The 2-degree deviation in this case is due to a fresh fuel asssembly on a major axis (H-15) of the core flats and once-burned assemblies in the other two locations in the flats region.

6.3. Capsule Fluence

Cumulative fast fluence at the center of the surveillance capsule was calculated to be 1.03 (+19) n/cm^2, 7% of which occurred in ANO-1 and 93% in Davis-Besse (Table 6-4). These data represent an average location in the capsule. In ANO-1, capsule AN1-A was located in an upper holder tube position at 11 degrees off the major axis and about 211 cm from the core center for 345 effective full power days (EFPD). It was then inserted in Davis-Besse in an upper holder tube position at 11 degrees off axis and about 202 cm from the core center for an additional 943 EFPD. During the latter irradiation period, the capsule was estimated to have been rotated approximately 90 degrees counterclockwise relative to its original design orientation (keyway facing the reactor core).

Babcock & Wilcox
a McDermott company

6.4. Fluence Uncertainties

Uncertainties were estimated for the fluence values reported herein. These data, Table 6-5, were based on comparisons to benchmark experiments when available, estimated and measured variations in input data, and engineering judgment. Because of the complexity of the fluence calculations, no comprehensive uncertainty limits exist for these results. The values in Table 6-5 represent a best estimate based on experience with these analyses.

Table 6-1. Surveillance Capsule Detectors

Detector reaction	Effective lower energy limit, MeV	Isotope half-life
$^{54}Fe(n,p)^{54}Mn$ (a)	2.5	312.5 days
$^{58}Ni(n,p)^{58}Co$ (a)	2.3	70.85 days
$^{238}U(n,f)^{137}Cs$ (a)	1.1	30.03 years
$^{237}Np(n,f)^{137}Cs$ (a)	0.5	30.03 years
$^{238}U(n,f)^{106}Ru$	1.1	369 days
$^{237}Np(n,f)^{106}Ru$	0.5	369 days
$^{238}U(n,f)^{103}Ru$	1.1	39.43 days
$^{237}Np(n,f)^{103}Ru$	0.5	39.43 days
$^{238}U(n,f)^{144}Ce$	1.1	284.4 days
$^{237}Np(n,f)^{144}Ce$	0.5	284.4 days
$^{238}U(n,f)^{95}Zr$	1.1	64.4 days
$^{237}Np(n,f)^{95}Zr$	0.5	64.4 days

(a)Due to the revised procedure for capsule flux determination, only these reactions were measured.

Babcock & Wilcox
a McDermott company

Table 6-2. Reactor Vessel Flux

	Fast flux, n/cm^2-s (E > 1 MeV)			Flux, n/cm^2-s (E > 0.1 MeV)
	Inside surface (max location)	T/4	3T/4	Inside surface (max location)
Cycle 1A[a] (345 EFPD)	1.39(+10)	7.9(+9)	1.8(+9)	2.68(+10)
Cycle 1B-4[a] (1047 EFPD)	1.46(+10)[b]	8.4(+9)[b]	1.9(+9)[b]	3.11(+10)[b]
Cycle 5 (447 EFPD)	1.03(+10)	5.9(+9)	1.3(+9)	2.15(+10)

[a]Capsule AN1-B analysis, B&W-1698.

[b]Due to ^{110m}Ag contamination of the fission dosimeter data, the measured activity of the detectors for the AN1-B capsule were determined to be 10% too large. Correcting for this contamination effect has reduced the normalization factor from1.07 to 0.95. Thus, the flux values listed for cycles 1B-4 above are about 11% lower than previously reported in BAW-1698.

Babcock & Wilcox
a McDermott company

Table 6-3. Reactor Vessel Fluence Gradient

Cumulative irradiation time	Fast fluence, n/cm^2 (E > 1.0 MeV)		
	Inside surface (max location)	T/4	3T/4
End of cycle 1A[a] (345 EFPD)	4.14(+17)	2.4(+17)	5.4(+16)
End of cycle 4[a] (1392 EFPD)	1.73(+18)[b]	9.8(+17)[b]	2.2(+17)[b]
End of cycle 5 (1839 EFPD)	2.13(+18)	1.2(+18)	2.8(+17)
8 EFPY	3.38(+18)	1.9(+18)	4.7(+17)
15 EFPY[c]	5.61(+18)	3.2(+18)	7.3(+17)
21 EFPY[d]	7.5(+18)	4.2(+18)	9.8(+17)
32 EFPY	1.10(+19)	6.3(+18)	1.4(+18)

[a]Capsule AN1-B analysis, BAW-1698.

[b]Reduced from values reported in BAW-1698, see (b) on Table 6-2 of this report.

[c]15 EFPY values are needed for T/2 and the outer surface; these values are 1.6(+18) and 2.9(+17), respectively.

[d]21 EFPY values are needed for T/2 and the outer surface; these values are 2.1(+18) and 3.9(+17), respectively.

Babcock & Wilcox
a McDermott company

Table 6-4. Surveillance Capsule Fluence

	Flux, n/cm^2-s (E > 1 MeV)	Fluence, n/cm^2	Cumulative fluence, n/cm^2
Method 1			
ANO-1, cycle 1A[a] (34⁵ EFPD)	2.44(+10)	7.27(+17)	7.27(+17)
Dav.. Besse Unit 1, cycle 1[a] (374 EFPD)	9.79(+10)	3.16 (+18)	3.89(+18)
Davis-Besse Unit 1, cycle 2[b] (296 EFPD)	9.67(+10)	2.61(+18)	6.50(+18)
Davis-Besse Unit 1, cycle 3 (273 EFPD)	1.54(+11)	3.62(+18)	1.01(+19)
Method 2			
ANO-1, cycle 1A (345 EFPD)	2.44(+10)	7.27(+17)	7.27(+17)
Davis-Besse Unit 1, cycle 1 (374 EFPD)	9.79(+10)	3.16(+18)	3.89(+18)
Davis-Besse Unit 1, cycles 2 and 3 (569 EFPD)	1.30(+11)	6.38(+18)	1.03(+19)
Method 3			
ANO-1, cycle 1A (345 EFPD)	2.44(+10)	7.27(+17)	7.27(+17)
Davis-Besse Unit 1, cycles 1, 2, and 3 (943 EFPD)	1.20(+11)	9.75(+18)	1.05(+19)

AVERAGE CUMULATIVE FLUENCE FROM 3 METHODS = 1.03(+19)

[a]Capsule AN1-B analysis, BAW-1698.

[b]Capsule RS1-D analysis, BAW-1792.[5]

Babcock & Wilcox
a McDermott company

Table 6-5. Estimated Fluenc Uncertainty

Calculated fluence	Estimated uncertainty	Basis of estimate
In the capsule	±18%	Activity measurements, cross sections, fission yields, saturation factor, and deviation from average fluence value.
In the reactor vessel at maximum location for cycle 5 of ANO-1	±24%	Activity measurements, cross sections, fission yields, saturation factors, axial factor, capsule location, radial/azimuthal extrapolation, and sigma of average normalization factor.
In the reactor vessel at the maximum location for end-of-life extrapolation	±26%	Items in vessel fluence above plus time/flux extrapolation to 32 EFPY.

Babcock & Wilcox
a McDermott company

Figure 6-1. Reactor Vessel Radial Flux/Fluence Gradient

Babcock & Wilcox
a McDermott company
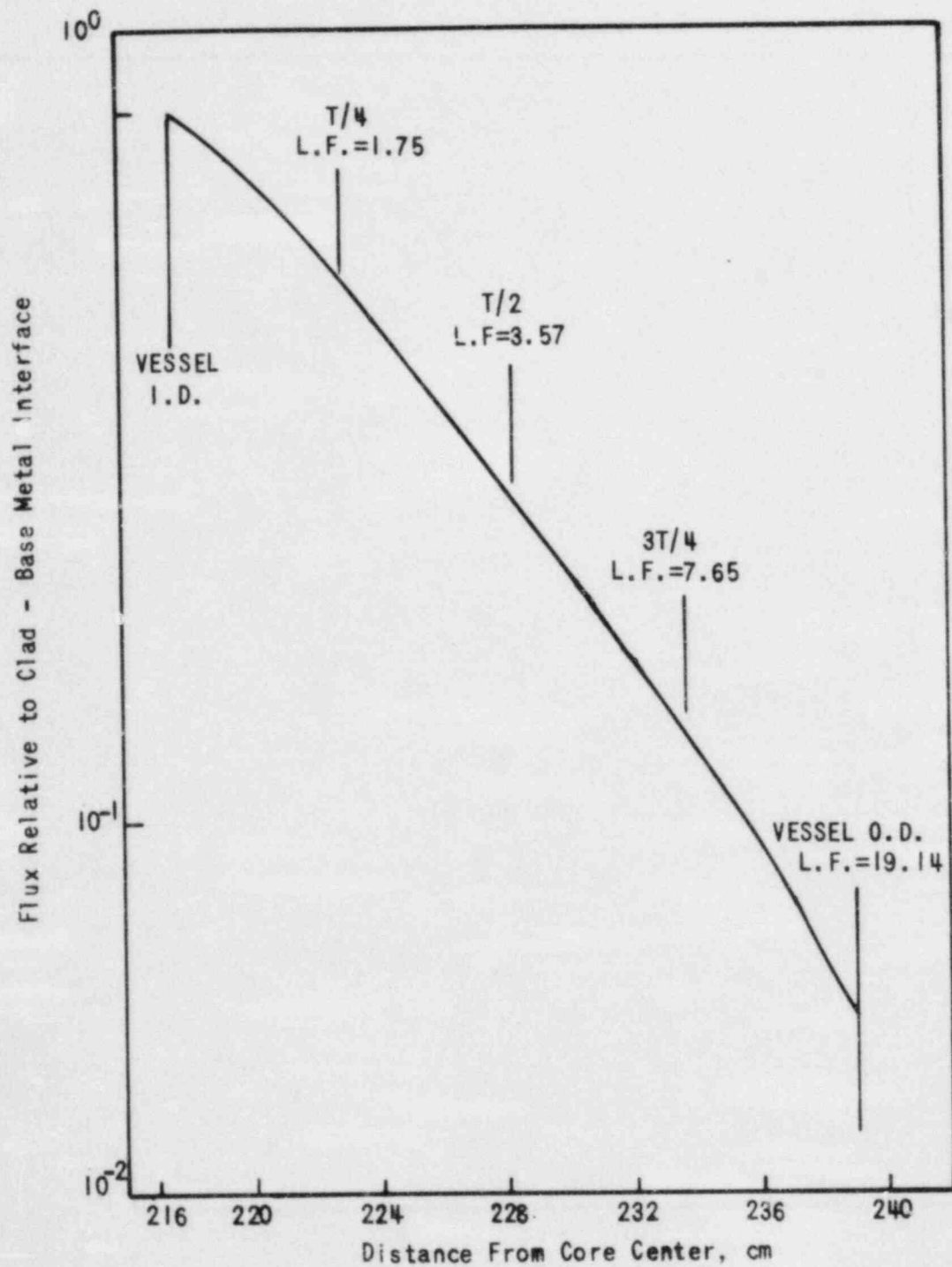
Figure 6-2. Azimuthal Flux Gradient (E > 1.0 MeV) at the Inside
Surface of the ANO-1 Reactor Vessel

Babcock & Wilcox
a M Dermott company
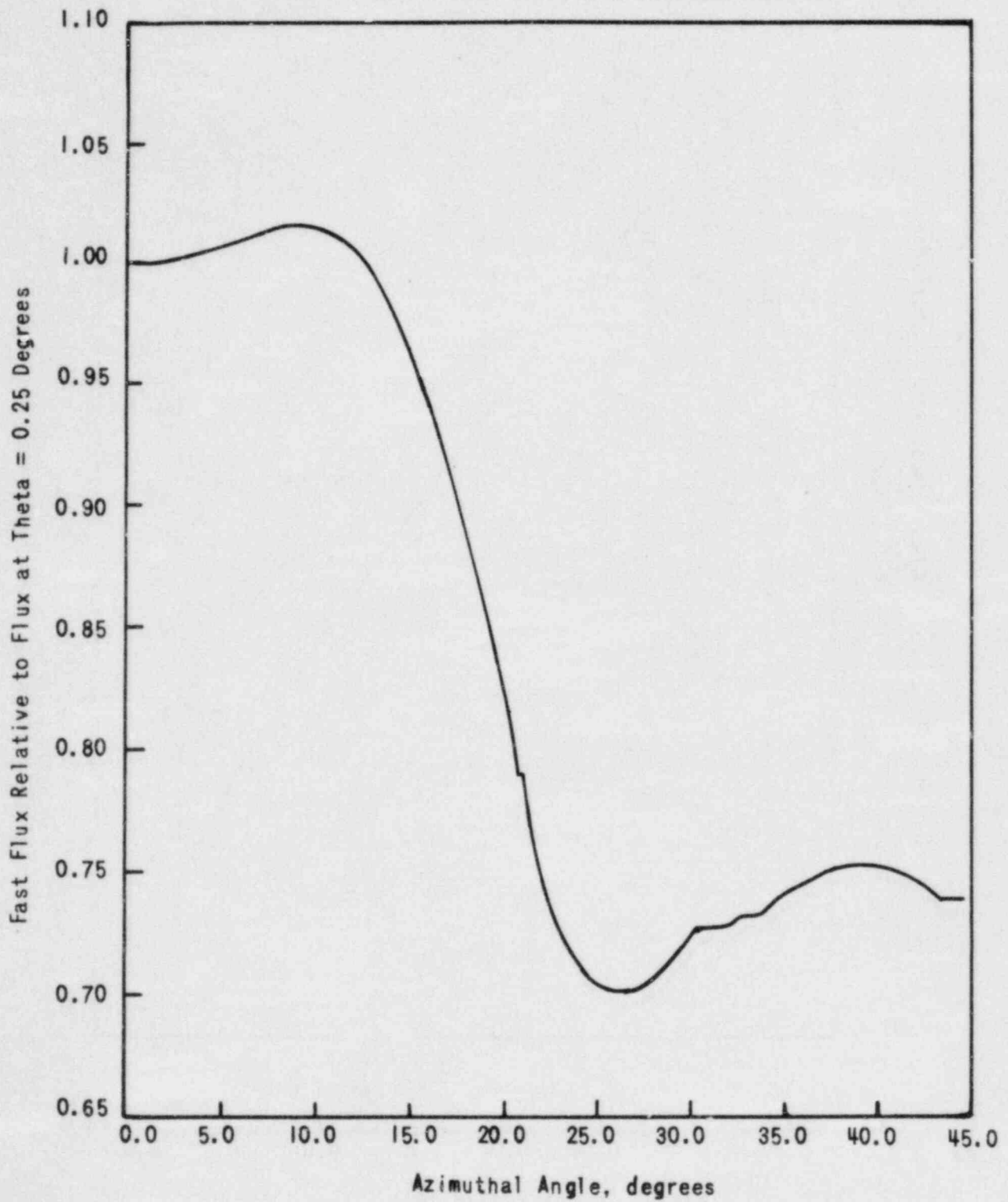
7. DISCUSSION OF CAPSULE RESULTS

7.1. Preirradiation Property Data

A review of the unirradiated properties of the reactor vessel core beltline region indicated no significant deviation from expected properties except in the case of the upper shelf properties of the weld metal. Based on the pre icted end-of-service peak neutron fluence value at the 1/4T vessel wall location and the copper content of the weld metal, it was predicted that the end-of-service Charpy upper shelf energies (USE) will be below 50 ft-lb. The weld metal selected for inclusion in the surveillance program was selected in accordance with the criteria in effect at the time the program was designed for ANO-1. The applicable selection criterion was based on the unirradiated properties only and before it was known that the weld metals are more sensitive to radiation damage than the base metal.

7.2. Irradiated Property Data

7.2.1. Tensile Properties

Table 7-1 compares irradiated and unirradiated tensile properties. At both room temperature and elevated temperature, the ultimate and yield strength changes in the base metal as a result of irradiation, and the corresponding changes in ductility are within the range of anticipated change. There appears to be some strengthening, as indicated by increases in ultimate and yield strength and similar decreases in ductility properties. All changes observed in the base metal are such as to be considered within acceptable limits. The change in the room temperature properties of the weld metal is greater than those observed for the base metal, indicating a greater sensitivity of the weld metal to irradiation damage. In either case, the changes in tensile properties are insignificant relative to the analysis of the reactor vessel materials at this period in service life.

Babcock & Wilcox
a McDermott company

A comparison of the tensile data from the first capsule (capsule AN1-E, fluence = 7.3E17 n/cm^2) with the corresponding data from the capsule reported in this report is shown in Table 7-2. The currently reported data came from specimens which experienced a fluence approximately 14 times greater than those from the first capsule. The general behavior of the tensile properties as a function of neutron irradiation is an increase in both ultimate and yield strengths and a decrease in ductility as measured by both total elongation and reduction in area. The most significant observation from these data is that the weld metal exhibited much greater sensitivity to neutron irradiation than did the base metal.

7.2.2. Impact Properties

The behavior of the Charpy V-notch impact data is more significant to the calculation of the reactor system's operating limitations. Table 7-3 compares the observed changes in irradiated Charpy impact properties with the predicted changes.

The shift in transition temperature was calculated for the surveillance materials using the predictive models in both Regulatory Guide (RG) 1.99, Revision 1, and the currently proposed revision to RG 1.99. Neither version specifies at which toughness level the prediction should be applied. The latest revision of 10 CFR 50, Appendix G specifies that the 30 ft-lb level of impact toughness should be used in determining the transition temperature shift, although past revisions specified the 50 ft-lb level.

The observed 30 ft-lb transition temperature shifts for all the surveillance materials are not in good agreement with the predicted shift values, with all the observed shifts being significantly less than the corresponding predicted shifts. The large degree of inaccuracy shown is due largely to the conservatisms built into each predictive model.

The observed 50 ft-lb transition temperature shifts for all the surveillance materials are not in good agreement with the predicted shift values, although the observed shifts were closer to the predicted values than the 30 ft-lb transition temperature shifts. The observed 35 MLE transition temperature shifts show no pattern from one material to another.

The observed decrease in Charpy USE with irradiation agreed with the predicted decrease fairly well for the longitudinal-oriented base metal, the weld metal, and the correlation material. The predicted decrease was very conservative in the case of the transverse-oriented base metal, and was non-conservative in the case of the HAZ material. The disagreement for the transverse base metal may be explained by a lack of transverse-oriented specimen data at the time the predictive model was developed, while HAZ material data often behaves in an erratic manner, probably due to the difficulty in machining the specimen notch in the same HAZ location from specimen to specimen. The agreement in USE decreases for the other three materials indicates that the predictive model is representative, not conservative.

A comparison of the Charpy impact data from the first two capsules (AN1-E and AN1-B) with the corresponding data from the capsule reported herein is shown in Table 7-4. The currently reported capsule experienced a fluence that is 14 times greater than capsule AN1-E, and 2-1/2 times greater than capsule AN1-B. The base metal and HAZ metal exhibited shifts at the 30 and 50 ft-lb levels for the current capsule that were larger than those of AN1-E. The 30 ft-lb levels had to be estimated for capsule AN1-E, but it appears that the 50 ft-lb shift increases were greater than the 30 ft-lb shift increases. For the current capsule, the weld metal exhibited a shift at the 30 ft-lb level which was larger than that of AN1-E. Interestingly, the observed shift was greater than the predicted shift for capsule AN1-E, whereas the reverse was true for the current capsule. The predictive model is now conservative for this weld.

For the current capsule, the correlation material exhibited a shift at the 50 ft-lb level which was larger than that of the first capsule and moderately larger than that of the second capsule. At 30 ft-lbs, the shift for the current capsule was slightly less than that of the second capsule. This indicates a saturation effect in this material at these fluence levels.

The longitudinal base metal, the HAZ material, and the weld metal all showed decreases in USE from capsule AN1-E. The transverse base metal did not decrease from AN1-E, possibly indicating a saturation effect, but more likely showing inaccuracy due to the limited number of specimens available in both cases. The correlation material did not show a significant decrease from capsule AN1-B, and this probably shows a saturation effect.

Babcock & Wilcox
a McDermott company

The lack of saturation in the other materials may be due to the large increase in fluence from capsule AN1-E to the current capsule; saturation may have been attained at an intermediate fluence.

Results from other surveillance capsules indicate that the RT_{NDT} estimating curves have greater inaccuracies than originally thought. These inaccuracies are a function of a number of parameters related to the basic data available at the time the estimating curves were established. Some of these include inaccurate fluence values, poor chemical composition values, and variations in data interpretation. The change in the regulations requiring the shift measurement to be based on the 30 ft-lb value may help to minimize errors that result from using the 30 ft-lb data base to predict the shift behavior at 50 ft-lbs.

The design curves for predicting the shift will be modified as more data become available; until that time, the design curves for predicting the RT_{NDT} shift as given in RG 1.99 are considered adequate for predicting the RT_{NDT} shift of those materials for which data are not available and will continue to be used to establish the pressure-temperature operational limitations for the irradiated portions of the reactor vessel until the time that new prediction curves are developed and approved.

Babcock & Wilcox
a McDermott company

Table 7-1. Comparison of Tensile Test Results

	Room temp test		Elevated temp test	
	Unirr	Irrad	Unirr	Irrad
Base Metal -- C 5114-1				
Fluence, 10^{18} n/cm^2 (E >1 MeV)	0	10.3	0	10.3
Ult tensile strength, ksi	94.8	99.7	91.8	94.8
0.2% yield strength, ksi	72.0	78.7	64.5	69.7
Uniform elongation, %	10	11	12	11
Total elongation, %	27	24	24	23
Reduction of area, %	68	55	64	61
Weld Metal -- WF 193				
Fluence, 10^{18} n/cm^2 (E >1 MeV)	0	10.3	0	10.3
Ult tensile strength, ksi	84.6	99.2	81.4	91.6
0.2% yield strength, ksi	67.6	84.1	60.4	73.2
Uniform elongation, %	12	12	11	10
Total elongation, %	28	24	22	19
Reduction of area, %	64	54	52	47

Table 7-2. Summary of ANO-1 Reactor Vessel Surveillance Capsules Tensile Test Results

Material	Fluence 10^{18} n/cm²	Test temp, F	Strength, ksi				Ductility, %			
			Ultimate	% Δ [a]	Yield	% Δ [a]	Total elongation	% Δ [a]	Reduction of area	% Δ [a]
Base metal	0	72	94.8	--	72.0	--	27	--	68	--
		570	91.8	--	64.5	--	24	--	64	--
	0.73	70	96.9	+2.2	75.6	+5.0	26	-3.7	67	-1.5
		570	95.3	+3.8	68.4	+6.0	22	-8.3	57	-10.9
	10.3	76	99.7	+5.2	78.7	+9.3	24	-11.1	55	-19.1
		580	94.8	+3.3	69.7	+8.1	23	-4.2	61	-4.7
Weld metal	0	72	84.6	--	67.6	--	28	--	64	--
		570	81.4	--	60.4	--	22	--	52	--
	0.73	70	91.3	+7.9	76.2	+12.7	24	-14.3	59	-7.8
		570	89.1	+9.5	68.8	+13.9	19	-13.6	47	-9.6
	10.3	75	99.2	+17.3	84.1	+24.4	24	-14.3	54	-15.6
		580	91.6	+12.5	73.2	+21.2	19	-13.6	47	-9.6

[a]Change relative to unirradiated.

Table 7-3. Observed Vs Predicted Changes in Irradiated Charpy Impact Properties

Transition Temperature Increase

Material	Observed shift in property, F			Predicted shift, F[a]	Predicted shift, F[b]
	30 ft-lb	50 ft-lb	35 MLE		
Base material (C5114-1)					
Transverse	66	70	63	122	140
Longitudinal	48	70	60	122	140
HAZ	45	90	18	122	140
Weld metal	151	ND[c]	129	284	243
Correlation material (HSST plate 02)	46	66	85	157	163

Charpy USE Decrease

Material	Decrease, ft-lb	
	Observed	Predicted[d]
Base material (C5114-1)		
Transverse	11	23
Longitudinal	24	32
HAZ	41	28
Weld metal	28	31
Correlation material (HSST plate 02)	35	34

[a]Per RG 1.99, Revision 1.

[b]Per draft revision of RG 1.99, based on shift plus 2σ margin.

[c]ND denotes not determinable.

[d]Per RG 1.99, Revision 1; no change of USE model in draft revision.

Table 7-4. Summary of ANO-1 Reactor Vessel Surveillance Capsules
Charpy Impact Test Results

Material	Fluence, 10^{18} n/cm^2	Transition temperature increase, F			Decrease in USE, ft-lb	
		30 ft-lb observed	50 ft-lb observed	Predicted[a]	Observed	Predicted[a]
Base material (C 5114-1)						
Longitudinal	0.73	30[b]	19	32	14	24
	10.30	48	70	122	24	32
Transverse	0.73	10[b]	22	32	14	19
	10.30	66	70	122	13	23
HAZ	0.73	13[b]	42	32	33	21
	10.30	45	90	122	41	28
Weld metal	0.73	115	137	76	15	15
	10.30	151	ND[c]	284	28	31
Correlation material (HSST plate 02)	0.73	12[b]	40	42	13	18
	4.28	50	57	101	34	28
	10.30	46	66	157	35	34

[a]Per RG 1.99, Revision 1.

[b]Estimated.

[c]ND denotes not determinable.

8. DETERMINATION OF REACTOR COOLANT PRESSURE BOUNDARY PRESSURE-TEMPERATURE LIMITS

The pressure-temperature limits of the reactor coolant pressure boundary (RCPB) of ANO-1 are established in accordance with the requirements of 10 CFR 50, Appendix G. The methods and criteria employed to establish operating pressure and temperature limits are described in topical report BAW-10046A.[6] The objective of these limits is to prevent nonductile failure during any normal operating condition, including anticipated operation occurrences and system hydrostatic tests. The following loading conditions are of interest:

1. Normal operations, including heatup and cooldown.
2. Inservice leak and hydrostatic tests.
3. Reactor core operation.

The major components of the RCPB have been analyzed in accordance with 10 CFR 50, Appendix G. The closure head region, the reactor vessel outlet nozzle, and the beltline region have been identified as the only regions of the reactor vessel, and consequently of the RCPB, that regulate the pressure-temperature limits. Since the closure head region is significantly stressed at relatively low temperatures (due to mechanical loads resulting from bolt preload), this region largely controls the pressure-temperature limits of the first several service periods. The reactor vessel outlet nozzle also affects the pressure-temperature limit curves of the first several service periods due to the high local stresses at the inside corner of the nozzle, which can be two to three times the membrane stresses of the shell. After the first several years of neutron radiation exposure, the RT_{NDT} of the beltline region materials will be high enough that the beltline region of the reactor vessel will start to control the pressure-temperature limits of the RCPB. For the service period for which the limit curves are established, the maximum allowable pressure as a function of fluid temperature is obtained through a point-by-point comparison of the

Babcock & Wilcox
a McDermott company

limits imposed by the closure head region, the outlet nozzle, and the belt-line region. The maximum allowable pressure is taken to be the lowest of three calculated pressures.

The limit curves for ANO-1 are based on the predicted values of the adjusted reference temperatures of all the beltline region materials at the end of the twenty-first EFPY; this time was selected because it is within the fluence value for the third capsule that confirmed the material behavior to be conservatively predicted by RG 1.99, Revision 1. Also, it is estimated that a fourth surveillance capsule will be withdrawn at the end of the refueling cycle when the estimated fluence corresponds to approximately 32 EFPY, which will confirm material behavior to reactor vessel end of life (EOL). The time difference between the withdrawal of the third and fourth surveillance capsules will be adequate for re-establishing the operating pressure and temperature limits for the final period of reactor vessel operation.

The unirradiated impact properties were determined for the surveillance beltline region materials in accordance with 10 CFR 50, Appendixes G and H. For the other beltline region and PCPB materials for which the measured properties are not available, the unirradiated impact properties and residual elements, as originally established for the beltline region materials, are listed in Table A-1. The adjusted reference temperatures are calculated by adding the predicted radiation-induced ΔRT_{NDT} and the unirradiated RT_{NDT}. The predicted ΔRT_{NDT} is calculated using the respective neutron fluence and copper and phosphorus contents. Figure 8-1 illustrates the calculated peak neutron fluence at several locations through the reactor vessel beltline region wall as a function of exposure time. The supporting information for Figure 8-1 is described in section 6. The neutron fluence values of Figure 8-1 are the predicted fluences that have been demonstrated (section 6) to be conservative. The design curves of RG 1.99* were used to predict the radiation-induced ΔRT_{NDT} values as a function of the material's copper and phosphorus content and neutron fluence.

- - - - -

*Revision 1, April 1977.

8-2

The neutron fluences and adjusted RT_{NDT} values of the beltline region materials at the end of the twenty-first EFPY are listed in Table 8-1. The neutron fluences and adjusted RT_{NDT} values are given for the 1/4T and 3/4T vessel wall locations. The assumed RT_{NDT} of the closure head region and the outlet nozzle steel forgings is 60F, in accordance with BAW-10046A. Figure 8-2 shows the reactor vessel's pressure-temperature limit curve for normal heatup. This figure also shows the core criticality limits as required by 10 CFR 50, Appendix G. Figures 8-3 and 8-4 show the vessel's pressure-temperature limit curve for normal cooldown and for heatup during inservice leak and hydrostatic tests, respectively. All pressure-temperature limit curves are applicable up to the twenty-first EFPY. Protection against nonductile failure is ensured by maintaining the coolant pressure below the upper limits of the pressure-temperature limit curves. The acceptable pressure and temperature combinations for reactor vessel operation are below and to the right of the limit curve. The reactor is not permitted to go critical until the pressure-temperature combinations are to the right of the criticality limit curve. To establish the pressure-temperature limits for protection against nonductile failure of the RCPB, the limits presented in Figures 8-2 through 8-4 must be adjusted by the pressure differential between the point of system pressure measurement and the pressure on the reactor vessel controlling the limit curves. This adjustment is necessary because the reactor vessel is the most limiting component of the RCPB.

Babcock & Wilcox
a McDermott company

Table 8-1. Data for Preparation of Pressure-Temperature Limit Curves for ANO-1 -- Applicable Through 21 EFPY

Material ident		Beltline region location	Weldment location			Unirr RT_{NDT}, F	Chemistry		Neutron fluence at end of 21 EFPY (E > 1 MeV), n/cm²		Radiation-induced ΔRT_{NDT} at end of 21 EFPY[a,b], F		Adjusted RT_{NDT} at end of 21 EFPY, F	
Heat No.	Type		Core midplane to weld CL, cm	Location from major axis, degrees	Weld 1/4T location		Copper content, %	Phosphorus content, %	At 1/4T	At 3/4T	At 1/4T	At 3/4T	At 1/4T	At 3/4T
AYN 131	SA508, Cl. 2	Nozzle belt	--	--	--	(+60)[c]	0.03	0.009	3.2E18	7.4E17	25	12	85	72
C 5120-2	SA533, Gr B	Upper shell	--	--	--	(+40)[c]	0.17	0.014	4.2E18	9.8E17	104	50	144	90
C 5114-2	SA533, Gr B	Upper shell	--	--	--	+10	0.15	0.010	4.2E18	9.8E17	78	38	88	48
C 5120-1	SA533, Gr B	Lower shell	--	--	--	+10	0.17	0.014	4.2E18	9.8E17	104	50	114	60
C 5114-1	SA533, Gr B	Lower shell	--	--	--	+30	0.15	0.010	4.2E18	9.8E17	78	38	108	68
WF 182-1	Weld	Upper circ. seam (100%)	123	--	Yes	+19	0.24[d]	0.014[d]	3.2E18	7.4E17	130	63	149	82
WF 112	Weld	Middle circ. seam (100%)	-63	--	Yes	0	0.31[d]	0.016[d]	4.2E18	9.8E17	201	97	201	97
SA 1788	Weld	Lower circ. seam (100%)	-249	--	Yes	(+20)[c]	0.25[d]	0.017[d]	2.3E16	5.5E15	12	6	32	26
WF 18	Weld	Upper long. (both 100%)	--	27.6	Yes	(+20)[c]	0.29[d]	0.010[d]	3.1E18	7.3E17	145	70	165	90
WF 18	Weld	Lower long. (both 100%)	--	56	Yes	(+20)[c]	0.29[d]	0.010[d]	3.3E18	7.6E17	140	72	169	92

[a]Per Regulatory Guide 1.99, Revision 1, April 1977.

[b]Regulatory Guide 1.99 not valid for shifts less than 50F.

[c]Per BAW-10046A, Revision 1, July 1977.

[d]Per BAW-1799, July 1983.

Figure 8-1. Predicted Fast Neutron Fluence at Various Locations Through Reactor Vessel Wall for First 21 EFPY

Figure 8-2. Reactor Vessel Pressure-Temperature Limit Curves for Normal Operation --
Heatup, Applicable for First 21 EFPY

Assumed RT$_{NDT}$, F		Point	Pressure, PSIG	Temp., F
Beltline Region 1/4T	201	A	457	70
Beltline Region 3/4T	97	B	457	135
Closure Head Region	60	C	625	219
Outlet Nozzle	60	D	625	250
		E	730	253
		F	1410	340
		G	2250	390
		H	1320	373
		I	2250	430

Applicable For Heatup Rates up to 100F/h

The acceptable pressure-temperature combinations are below and to the right of the limit curve(s). The Limit curves do not include the pressure differential between the point of the system pressure measurement and the pressure on the reactor vessel region controlling the limit curve, nor do they include any additional margin of safety for possible instrument error.

Criticality Limit

Figure 8-3. Reactor Vessel Pressure-Temperature Limit Curve for Normal
Operation -- Cooldown, Applicable for First 21 EFPY

The acceptable pressure-temperature combinations are below and to
the right of the limit curve(s). The limit curves do not include
the pressure differential between the point of system pressure
measurement and the pressure on the reactor vessel region controlling
the limit curve, nor do they include any additional margin of safety
for possible instrument error.

Assumed RT_{NDT}, F

Beltline Region 1/4T	201
Beltline Region 3/4T	97
Closure Head Region	60
Outlet Nozzle	60

Point	Pressure, PSIG	Temp., F
A	300	70
B	648	225
C	1390	305
D	2250	353

Applicable for
Cooldown Rates
Up to 100F/h

Figure 8-4. Reactor Vessel Pressure-Temperature Limit Curve for Inservice Leak and Hydrostatic Tests, Applicable for First 21 EFPY

Assumed RT_{NDT}, F

Beltline Region 1/4T	201
Beltline Region 3/4T	97
Closure Head Region	60
Outlet Nozzle	60

Point	Pressure PSIG	Temp., T
A	400	70
B	521	130
C	525	175
D	625	225
E	871	230
F	1563	320
G	2500	371

Applicable For Heatup and Cool-down Rates up to $\leq$100F/h ($\leq$50F in any 1/2-h Period)

The acceptable pressure-temperature combinations are below and to the right of the limit curve(s). The limit curves do not include the pressure differential between the point of system pressure measurement and the pressure on the reactor vessel region controlling the limit curve, nor do they include any additional margin of safety for possible instrument error.

Reactor Vessel Coolant Pressure, psig

Reactor Vessel Coolant Temperature, F

9. SUMMARY OF RESULTS

The analysis of the reactor vessel material contained in the third surveillance capsule, AN1-A, removed for evaluation as part of the ANO-1 reactor vessel surveillance program, led to the following conclusions:

1. The capsule received an average fast fluence of 1.03×10^{19} n/cm^2 (E > 1.0 MeV). The predicted fast fluence for the ANO-1 reactor vessel 1/4T location at the end of the fifth fuel cycle is 1.2×10^{18} n/cm^2 (E > 1 MeV).

2. The fast fluence of 1.03×10^{19} n/cm^2 (E > 1 MeV) increased the RT$_{NDT}$ of the AN1-A capsule reactor vessel core region shell materials a maximum of 151F.

3. Based on the calculated fast flux at the vessel wall, an 80% load factor, and the planned fuel management, the projected fast fluence that the ANO-1 reactor pressure vessel will receive in 40 calendar years' operation is 1.10×10^{19} n/cm^2 (E > 1 MeV).

4. The increase in the RT$_{NDT}$ for the base plate material was not in good agreement with that predicted by the currently used design curves of ΔRT$_{NDT}$ versus fluence, but the prediction techniques are conservative.

5. The increase in the RT$_{NDT}$ for the weld metal was not in good agreement with that predicted by the currently used design curves of ΔRT$_{NDT}$ versus fluence, but the prediction techniques are conservative.

6. The current techniques used for predicting the change in weld metal Charpy impact upper shelf properties due to irradiation are conservative.

7. The comparison of changes in transition temperature and USE with those of previous surveillance capsules indicates that a saturation effect with fluence may be occurring. Further data are required before this can be stated definitively.

Babcock & Wilcox
a McDermott company

8. The analysis of the neutron dosimeters demonstrated that the analytical techniques used to predict the neutron flux and fluence were accurate.

9. The capsule design operating temperature may have been exceeded during operating transients but not for times and temperatures that would preclude the use of the capsule data.

10. SURVEILLANCE CAPSULE REMOVAL SCHEDULE

Based on the postirradiation test results of capsule AN1-A, the following schedule is recommended for examination of the remaining capsules in the ANO-1 RVSP:

Capsule ID	Evaluation schedule[a]			
	Est. capsule fluence, 10^{19} n/cm^2	Est. vessel fluence, 10^{19} n/cm^2		Est. date data available[b]
		Surface	1/4T	
AN1-C	1.4	0.32	0.18	1986
AN1-D[c]	1.4	0.45	0.25	1990
AN1-F[c]	1.4	0.52	0.29	1992

[a]In accordance with BAW-10006A[3] and E 185-82 as modified by BAW-1543, Rev. 2.[4]
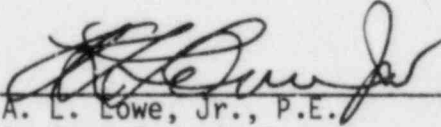
[b]Estimated date based on 0.8 plant operation factor.

[c]Capsules designated as standbys which may not be evaluated.

Babcock & Wilcox
a McDermott company
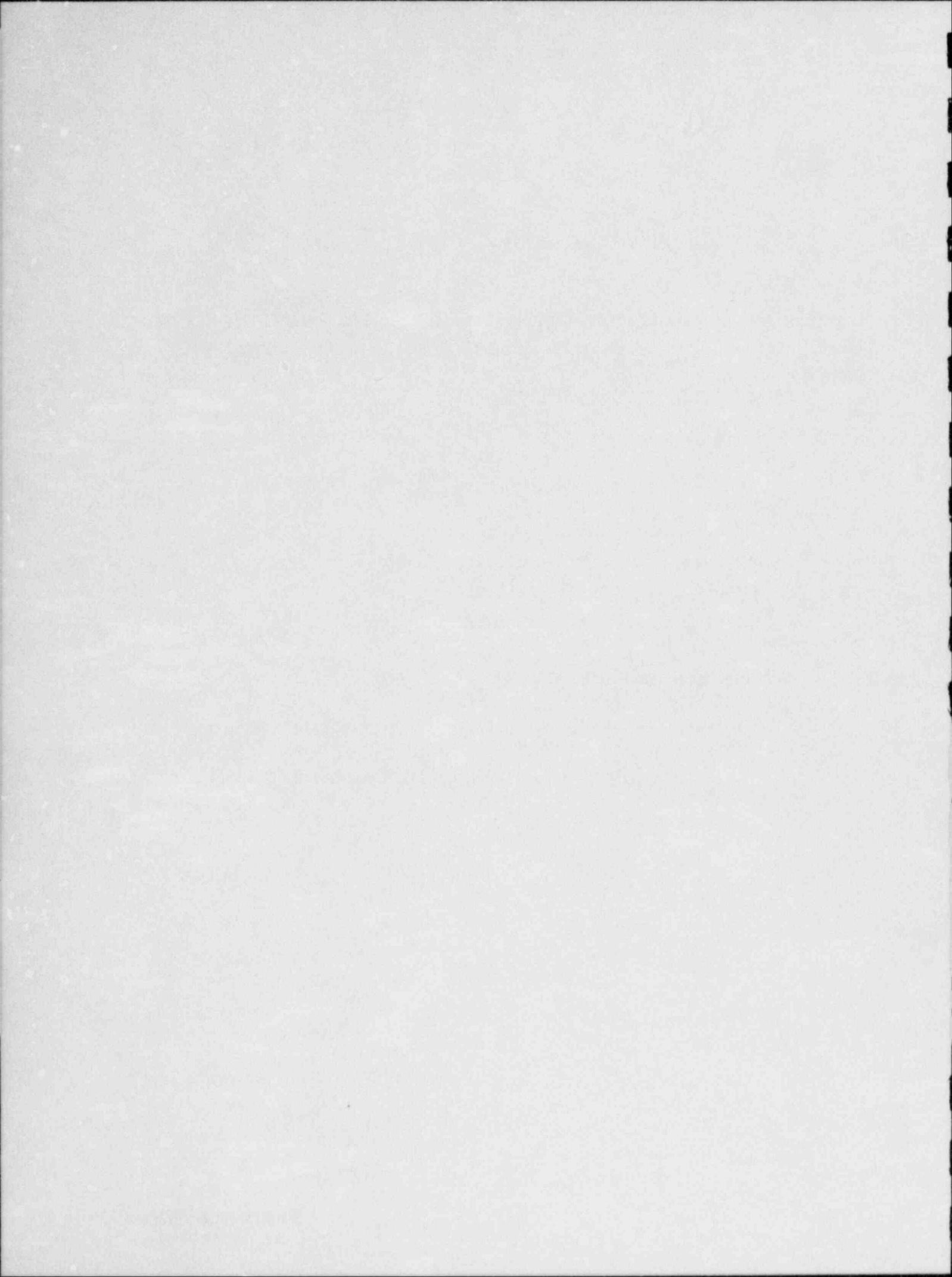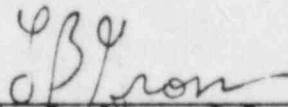
11. CERTIFICATION

The specimens were tested, and the data obtained from Arkansas Nuclear One, Unit 1 surveillance capsule AN1-A were evaluated using accepted techniques and established standard methods and procedures in accordance with the requirements of 10 CFR 50, Appendixes G and H.

A. L. Lowe, Jr., P.E.   24 July 1984
                                          Date
Project Technical Manager

This report has been reviewed for technical content and accuracy.

L. B. Gross, P.E.   July 24, 1984
                                          Date
Materials and Chemical
Engineering Services

APPENDIX A

Reactor Vessel Surveillance Program --
Background Data and Information

1. Material Selection Data

The data used to select the materials for the specimens in the surveillance program, in accordance with E 185-66, are shown in Table A-1. The locations of these materials within the reactor vessel are shown in Figures A-1 and A-2.

2. Definition of Beltline Region

The beltline region of ANO-1 was defined in accordance with the data given in BAW-10006A.[3]

3. Capsule Identification

The capsules used in the ANO-1 surveillance program are identified below by identification number, type, and location.

Capsule Cross Reference Data

Number	Type
AN1-A	I
AN1-B	II
AN1-C	I
AN1-D	II
AN1-E	I
AN1-F	II

4. Specimens per Surveillance Capsule

See Tables A-2, A-3, and A-4.

Babcock & Wilcox
a McDermott company

Table A-1. Unirradiated Impact Properties and Residual Element Content Data of Beltline Region Materials Used for Selection of Surveillance Program Materials -- ANO-1

Material ident, heat No.	Material type	Beltline region location	Distance, core midplane to weld centerline, cm	Drop wt, T_{NDT}, F	Charpy data, CVN[a] Longitudinal At 10F ft-lb	Transverse 50 ft-lb, F	35 MLE, F	USE, ft-lb	RT_{NDT}, F	Chemistry, %[b] Cu	P	S	Ni
AYN131	SA508, Cl 2	Nozzle belt	--	--	{74,83,61 / 41,58,68}	--	--	--	--	0.05	0.013	0.020	0.68
C 5120-2	SA533, Gr B	Upper shell	--	--	67,63,59	--	--	--	--	0.17	0.014	⌐.013	0.55
C 5114-2[c]	SA533, Gr B	Upper shell	--	--	31,34,35	--	--	--	--	0.15	0.010	0.016	0.52
C 5120-1	SA533, Gr B	Lower shell	--	--	53,56,54	--	--	--	--	0.17	0.014	0.013	0.55
C 5114-1[d]	SA533, Gr B	Lower shell	--	--	21,57,21	--	--	--	--	0.15	0.010	0.016	0.52
WF 182-1	Weld	Upper circum	123	--	36,33,44	--	--	--	--	0.18	0.014	0.015	0.59
WF 112	Weld	Middle circum	-63	--	35,40,30	--	--	--	--	0.22	0.024	0.006	0.58
SA1788	Weld	Lower circum	-249	--	40,38,36	--	--	--	--	0.29	0.017	0.012	0.47
WF 18	Weld	{Upper longit / Lower longit}	--	--	45,46,38	--	--	--	--	0.105	0.004	0.017	0.45
WF 193[e]	Weld	Surveillance weld	--	--	29,30,37	--	--	--	--	0.19	0.016	0.008	0.59

[a] CVN denotes Charpy V-notch.

[b] From mill and qualification test reports.

[c] Surveillance base metal A.

[d] Surveillance base metal B.

[e] Surveillance weld metal.

Table A-2.   Test Specimens for Determining
Material Baseline Properties

| | No. of test specimens | | |
| | Tensile | | |
Material description	70F	570F[a]	Charpy
Heat GG (C 5114-1)			
Base metal			
Transverse direction	3	3	26
Longitudinal direction	3	3	27
HAZ			
Transverse direction	3	2	27
Longitudinal direction	3	3	26
Total	12	11	106
Heat HH (C 5114-2)			
Base metal			
Transverse direction	3	3	27
Longitudinal direction	3	3	27
HAZ			
Transverse direction	3	3	27
Longitudinal direction	3	3	26
Total	12	12	107
Weld metal			
Longitudinal direction	3	3	27

A-4

Table A-3. Specimens in Upper Surveillance Capsules
(Designations A, C, and E)

Material description	No. of test specimens	
	Tensile	Charpy
Weld metal, WF 193	4	8
HAZ A, heat No. C 5114-1, longitudinal	0	8
Base material -- Plate A, Heat No. C 5114-1: longitudinal	4	8
transverse	0	4
Correlation, HSST plate 02	0	8
Total per capsule	8	36

Table A-4. Specimens in Lower Surveillance Capsules
(Designations B, D, and F)

Material description	No. of test specimens	
	Tensile	Charpy
HAZ B, Heat No. C 5114-2, longitudinal	4	10
Base material -- Plate B, Heat No. C 5114-2: longitudinal	4	10
transverse	0	8
Correlation, HSST plate 02	0	8
Total per capsule	8	36

A-5

Babcock & Wilcox
a McDermott company

Figure A-1. Location and Identification of Materials
Used in Fabrication of ANO-1, Reactor
Pressure Vessel

A-6
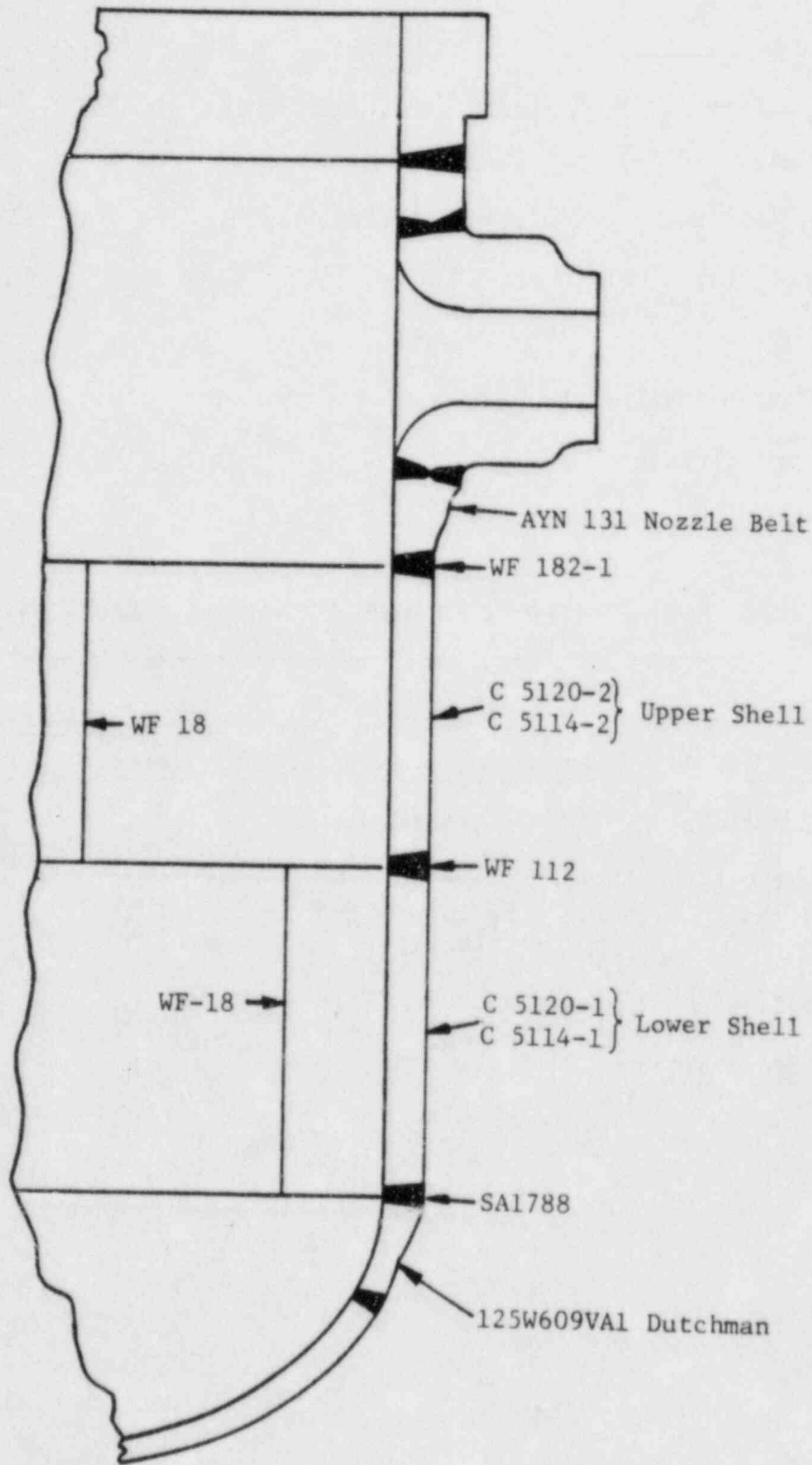
Figure A-2. Location of Longitudinal Welds in
Upper and Lower Shell Courses

Babcock & Wilcox
a McDermott company
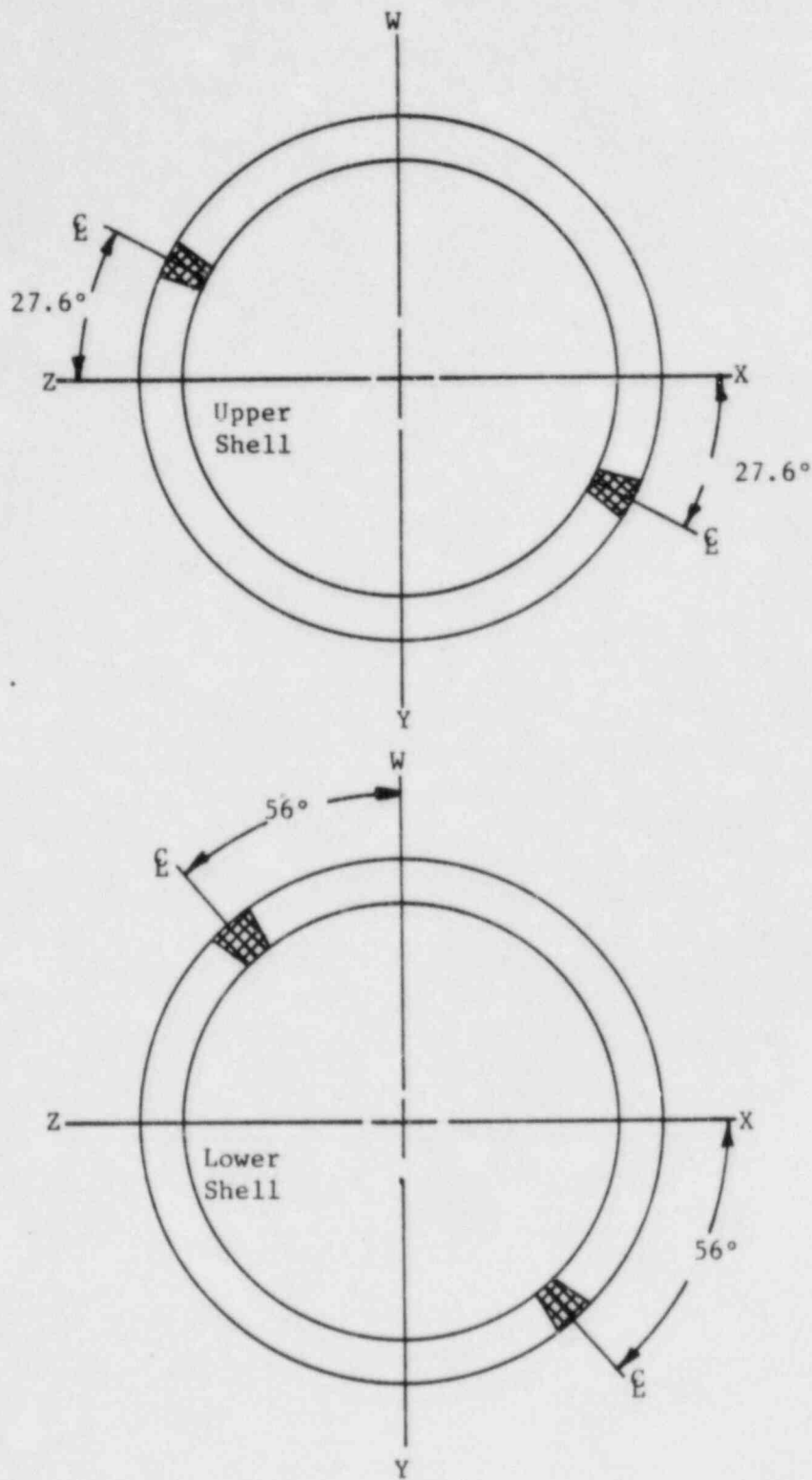
APPENDIX B
Preirradiation Tensile Data

Table B-1. Tensile Properties of Unirradiated Shell
Plate Material, Heat No. C 5114-1

Specimen No.	Test temp, F	Strength, psi		Elongation, %		Red'n of area, %
		Yield	Ultimate	Uniform	Total	
Longitudinal						
GG-708	RT	71,430	94,500	10.3	27.9	68.8
GG-711	RT	72,870	94,930	8.3	26.4	68.5
GG-717	RT	71,590	94,120	11.3	26.7	67.3
Mean	RT	71,960	94,850	10.0	26.7	68.2
Std dev'n		790	320	1.5	1.1	0.8
GG-704	570	64,110	91,160	11.2	22.9	63.6
GG-705	570	64,220	92,070	12.8	25.7	63.6
GG-715	570	65,290	92,270	12.0	24.3	64.9
Mean	570	64,540	91,830	12.0	24.3	64.0
Std dev'n		650	590	0.8	1.4	0.8

Table B-2. Tensile Properties cf Unirradiated
Weld Metal, WF 193

Specimen No.	Test temp, F	Strength, psi		Elongation, %		Red'n of area, %
		Yield	Ultimate	Uniform	Total	
GG-101	RT	67,800	84,850	13.3	28.6	64.7
GG-105	RT	67,790	84,980	10.8	27.1	62.9
GG-114	RT	67,080	84,040	12.7	28.6	64.3
Mean	RT	67,560	84,620	12.2	28.1	64.0
Std dev'n		410	510	1.23	0.9	1.0
GG-102	570	62,390	82,400	9.9	21.4	51.1
GG-109	570	59,110	80,850	11.4	22.1	50.4
GG-112	570	59,640	80,870	11.2	22.1	54.7
Mean	570	60,380	81,370	10.8	21.9	52.1
Std dev'n		1,760	890	0.8	0.4	2.3

Babcock & Wilcox
a McDermott company

APPENDIX C
Preirradiation Charpy Impact Data

Babcock & Wilcox
a McDermott company

Table C-1. Charpy Impact Data From Unirradiated Base Material, Longitudinal Orientation, Heat No. C 5114-1

Specimen No.	Test temp, F	Absorbed energy, ft-lb	Lateral expansion, 10^{-3} in.	Shear fracture, %
GG-707	319	132	68	100
708	319	131	68	100
741	319	124	67	100
GG-703	199	136	66	100
735	199	130	60	100
717	198	124	64	100
GG-748	142	136	69	100
747	140	129	65	100
756	140	136	68	100
GG-744	86	108	64	80
732	85	108	61	82
706	85	104	57	75
GG-745	50	70	48	25
751	50	82	57	30
752	50	102	63	45
GG-749	36	68	48	18
750	35	73	49	15
755	35	71	51	12
GG-754	20	21	16	2
753	20	30	21	3
746	19	53	38	5
GG-733	0.9	48	32	4
724	0.3	43	30	2
704	0.3	60	43	8
GG-736	-39	46	31	3
739	-39	37	24	2
722	-39	15	8.5	0

Babcock & Wilcox
a McDermott company

Table C-2. Charpy Impact Data From Unirradiated Base Material, Transverse Orientation, Heat No. C 5114-1

Specimen No.	Test temp, F	Absorbed energy, ft-lb	Lateral expansion, 10^{-3} in.	Shear fracture, %
GG-603	320	88	62	100
605	319	84	60	100
618	322	94	64	100
GG-632	259	91	61	100
638	259	94	63	100
640	258	92	61	100
GG-610	200	86	58	100
616	200	96	58	100
624	200	101	60	100
GG-634	141	89	60	94
639	140	90	61	100
633	138	100	61	97
GG-631	111	66	46	75
636	111	53	43	45
630	110	80	55	70
GG-626	80	54	40	35
612	80	56	42	45
607	79	48	32	30
GG-637	61	60	42	30
635	61	38	29	20
629	60	64	44	45
GG-625	30	37	32	2
GG-614	30	32	24	1
GG-608	-38	28	16	1
620	-40	28	16	1
613	-40	14	5	0

Table C-3. Charpy Impact Data From Unirradiated Base Metal, HAZ, Longitudinal Orientation, Heat No. C 5114-1

Specimen No.	Test temp, F	Absorbed energy, ft-lb	Lateral expansion, 10^{-3} in.	Shear fracture, %
GG-423	321	83	62	100
434	320	96	58	100
438	320	83	57	100
GG-447	205	104	56	100
445	202	116	59	100
449	198	123	63	100
GG-453	142	107	63	100
450	140	95	54	100
448	140	107	58	100
GG-426	81	70	44	100
420	80	74	44	94
403	80	84	46	100
GG-452	56	79	43	100
446	55	77	42	90
455	54	73	45	92
GG-451	46	86	44	94
456	45	69	43	98
GG-412	31	52	33	35
417	30	66	35	85
422	30	46	33	65
GG-411	-10	43	21	65
444	-10	40	21	30
418	-10	53	31	18
GG-433	-38	32	18	18
419	-39	32	17	15
425	-39	44	25	12

Babcock & Wilcox
a McDermott company

Table C-4. Charpy Impact Data From Unirradiated
Weld Metal, WF 193

Specimen No.	Test temp, F	Absorbed energy, ft-lb	Lateral expansion, 10^{-3} in.	Shear fracture, %
GG-011	320	77	59	100
044	320	73	61	100
035	319	70	60	100
GG-023	201	76	49	100
006	200	72	52	100
031	200	66	55	100
GG-055	141	67	55	96
051	140	67	46	97
049	139	71	53	100
GG-050	109	7	51	97
056	109	b7	59	82
045	108	64	46	85
GG-001	87	63	52	75
021	82	56	48	65
034	82	50	38	55
GG-053	60	35	32	20
047	60	28	25	25
046	60	49	38	55
GG-005	30	42	35	28
012	29	38	29	40
024	29	42	42	38
GG-052	1	16	14	8
054	1	33	25	10
048	0	37	31	6
GG-028	-38	22	15	4
013	-39	12	9	2
027	-39	20	12	3

Babcock & Wilcox
a McDermott company

Figure C-1. Charpy Impact Data for Unirradiated Base Metal,
Longitudinal Orientation

Babcock & Wilcox
a McDermott company
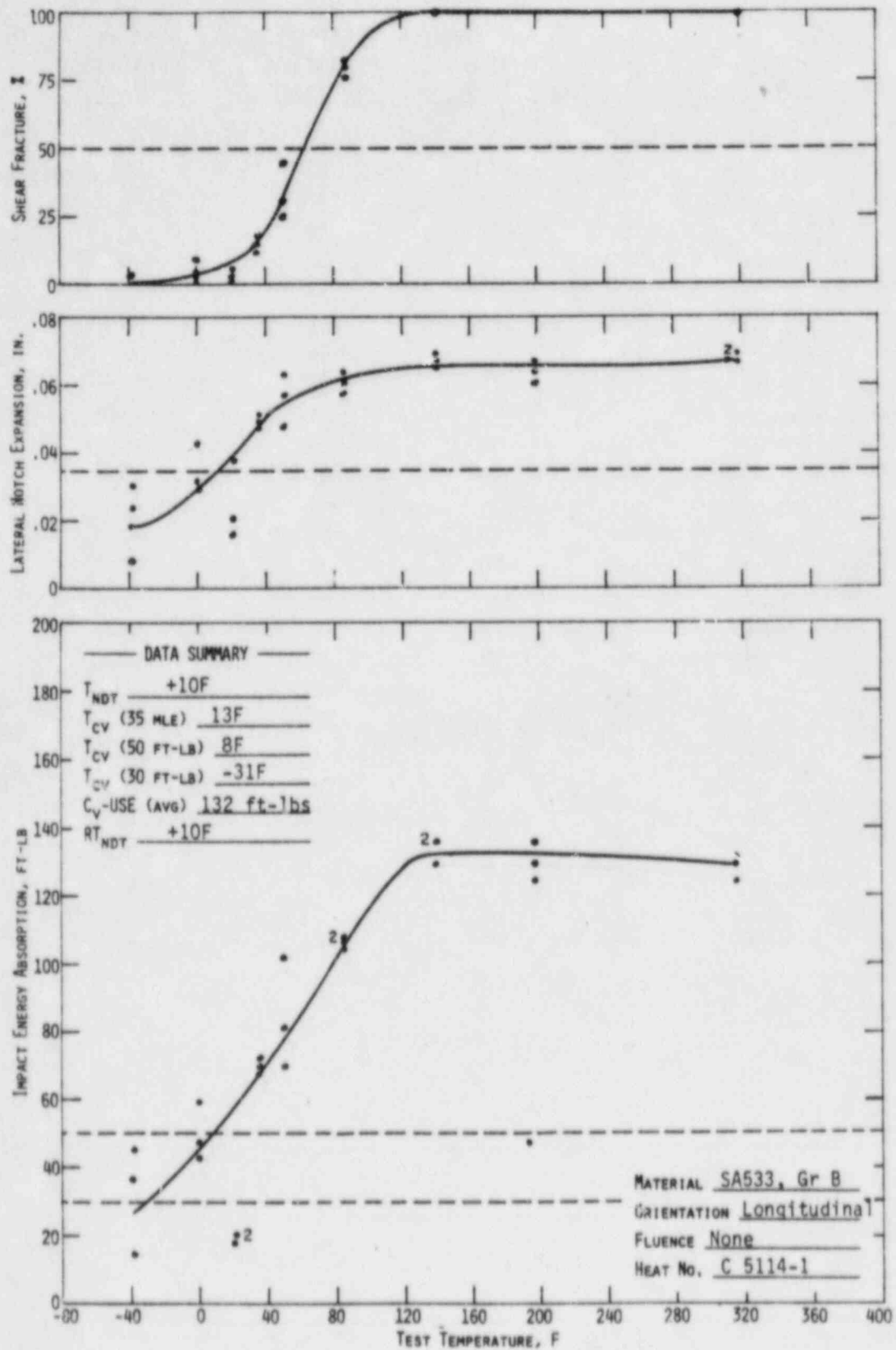
Figure C-2.   Charpy Impact Data for Unirradiated Base Metal,
Transverse Orientation
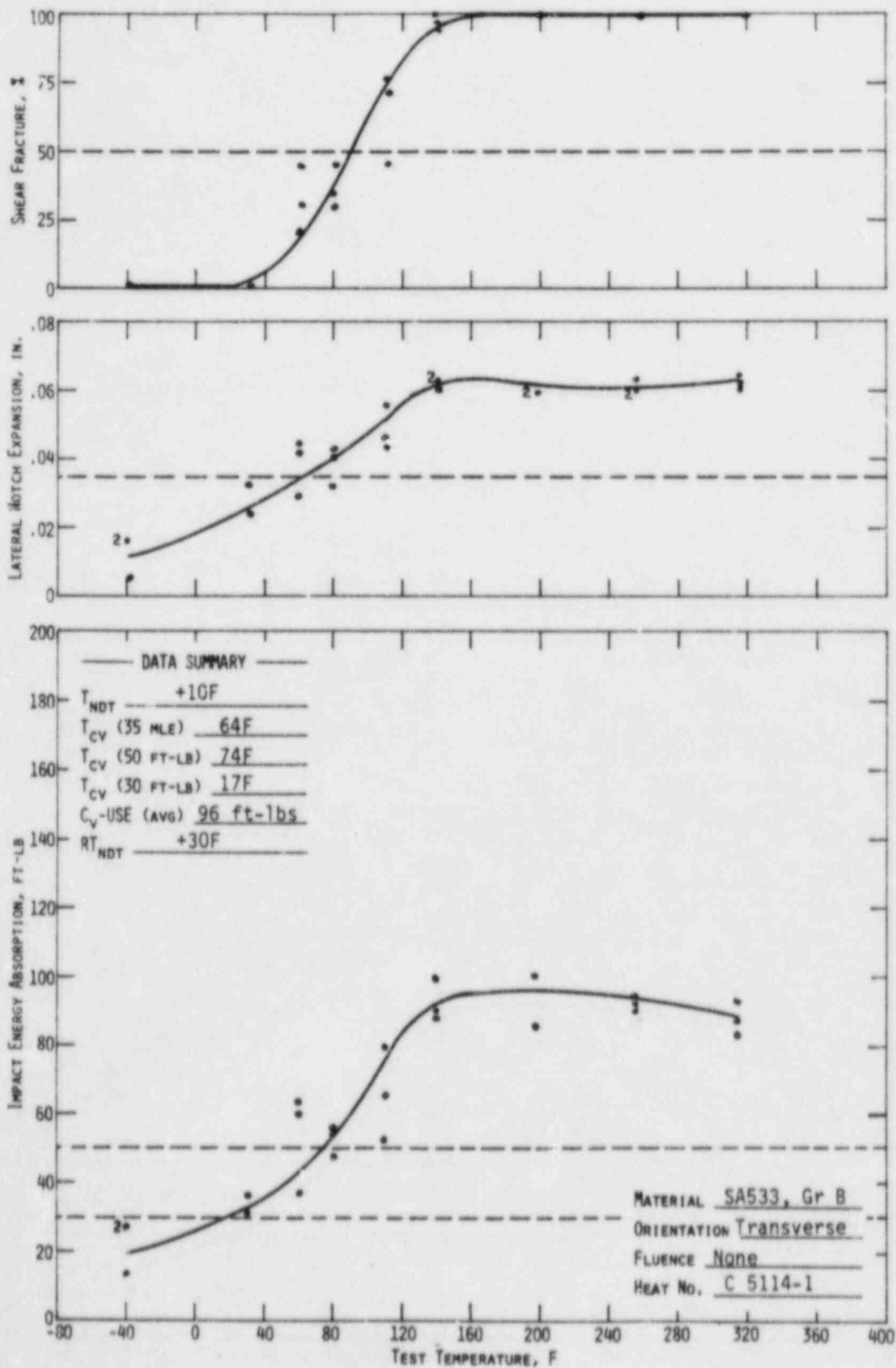
DATA SUMMARY

T_{NDT} — +10F
T_{CV} (35 MLE) 64F
T_{CV} (50 FT-LB) 74F
T_{CV} (30 FT-LB) 17F
C_V-USE (AVG) 96 ft-lbs
RT_{NDT} +30F

MATERIAL SA533, Gr B
ORIENTATION Transverse
FLUENCE None
HEAT No. C 5114-1

Babcock & Wilcox
a McDermott company

Figure C-3. Charpy Impact Data for Unirradiated Base Metal,
HAZ, Longitudinal Orientation

DATA SUMMARY

T_{NDT} ___-40F___

T_{CV} (35 MLE) ___42F___

T_{CV} (50 FT-LB) ___0F___

T_{CV} (30 FT-LB) ___-43F___

C_V-USE (AVG) ___115 ft-lbs___

RT_{NDT} ___0F___

MATERIAL ___SA533, Gr B___

ORIENTATION ___HAZ -- Long.___

FLUENCE ___None___

HEAT No. ___C 5114-1___

Babcock & Wilcox
a McDermott company
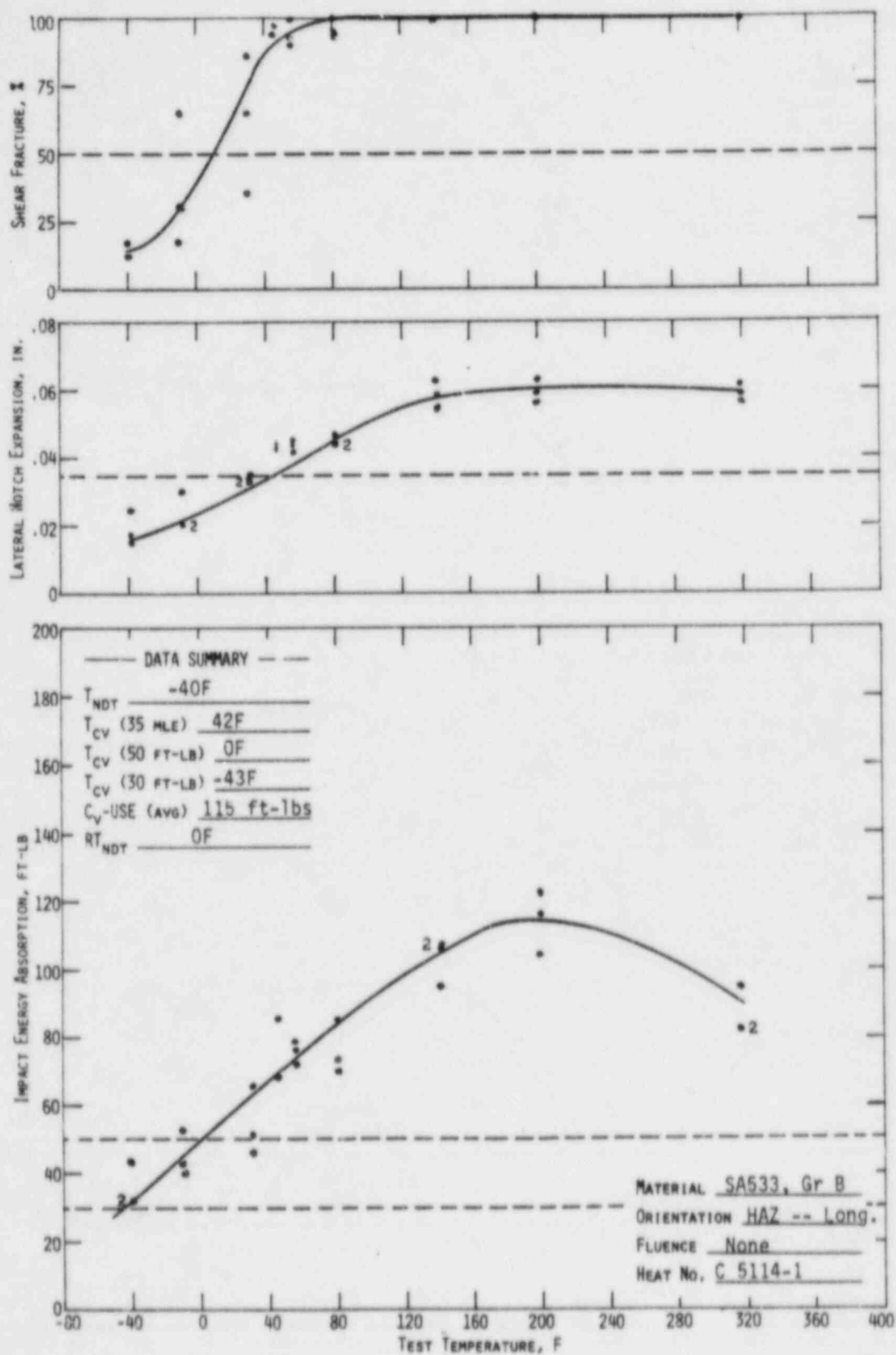
Figure C-4. Charpy Impact Data for Unirradiated Weld Metal

DATA SUMMARY

T_{NDT} __-20F__
T_{CV} (35 MLE) __65F__
T_{CV} (50 FT-LB) __65F__
T_{CV} (30 FT-LB) __5F__
C_V-USE (AVG) __73 ft-lbs__
RT_{NDT} __30F__

MATERIAL __Weld metal__
ORIENTATION ____
FLUENCE __None__
HEAT No. __WF 193__

C-9

Babcock & Wilcox
a McDermott company
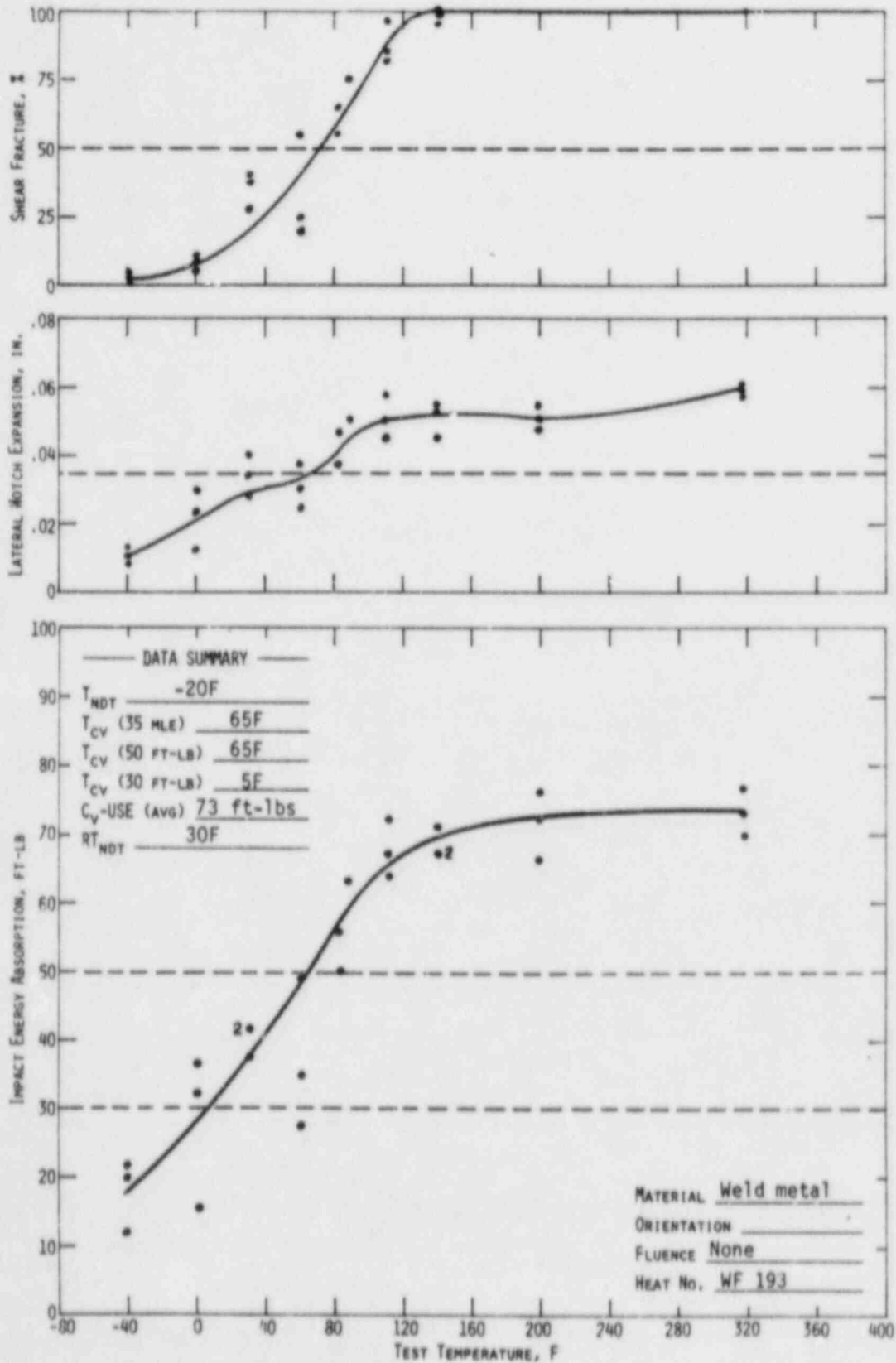
APPENDIX D
Fluence Analysis Procedures

1. Analytical Method

The procedure used in this analysis differs from previous procedures in two significant aspects: the calculation of the capsule flux and the normalization factor. Previous analyses calculated the capsule flux using the DOT4[7] code with an explicit model of the capsule. This flux was then used in equation D-1 to obtain a calculated activity for each dosimeter. A factor, defined as the measured activity divided by the calculated activity, was then calculated and used to normalize the calculated capsule and vessel flux to measured results. Use of this procedure in a series of capsule analyses has resulted in a fairly consistent average normalization factor of 0.95 from the $^{238}U(n,f)^{137}Cs$ and $^{237}Np(n,f)^{137}Cs$ reactions. In addition, these analyses have produced a consistent set of spectrum-averaged reaction cross sections as a function of capsule position, i.e., 11 or 26 degrees azimuthally. Based on the consistency of the normalization factor and the cross sections, a revised analysis procedure was developed. Basically, the procedure involves calculating the capsule flux from equation D-6 using the measured activities and the spectrum-averaged cross sections. The vessel flux still is calculated with DOT4, but the flux is normalized using the average normalization factor from previous analyses. A more detailed description of this revised procedure is given below.

1.1. Capsule Flux and Fluence Calculation

Preivous capsule analyses employed the DOT4 code, including an explicit model of the capsule assembly, to calculate the neutron flux as a function of energy in the capsule. The calculated fluxes were used in the following equation to obtain calculated activities for comparison with the measured data. The calculated activity for reaction product i, D_i, ($\mu Ci/gm$) is:

$$D_i = \frac{N}{A_n} \frac{1}{3.7 \times 10^4} f_i \sum_E \sigma_n(E)\phi(E) \sum_{j=1}^{M} F_j(1 - e^{-\lambda_i t_j})e^{-\lambda_i(T-\tau_j)} \qquad (D-1)$$

where
$\quad$ N = Avogadro's number,

$\quad$ A_n = atomic weight of target material n,

$\quad$ f_i = either weight fraction of target isotope in nth material or the fission yield of the desired isotope,

Babcock & Wilcox
a McDermott company

$\sigma_n(E)$ = group-averaged cross sections for material n (listed in Table E-3),

$\phi(E)$ = group-averaged fluxes calculated by DOT4 analysis,

F_j = fraction of full power during jth time interval, t_j,

λ_i = decay constant of the ith isotope,

t_j = interval of power history,

T = sum of total irradiation time, i.e., residual time in reactor, and wait time between reactor shutdown and counting,

τ_j = cumulative time from reactor startup to end of jth time period,

The normalization factor that was applied to the calculated flux was obtained from the ratio of the measured to calculated activities, i.e.,

$$C = \frac{D_i \text{ (measured)}}{D_i \text{ (calculated)}} . \tag{D-2}$$

Equation D-1 can be abbreviated as:

$$D_i = K_i P_i \sum_E \sigma_n(E)\phi(E) \tag{D-3}$$

where K_i contains the constant terms and P_i is the summation over j representing the power (saturation) term.

Given the energy-dependent flux from DOT4 and the energy-dependent cross sections, an average reaction cross section for E greater than 1 MeV can be found from

$$\bar{\sigma}_n = \frac{\sum \sigma_n(E)\phi(E)}{\sum \phi(E)} . \tag{D-4}$$

Then, equation D-3 becomes

$$D_i = K_i P_i \bar{\sigma}_n \quad (E > 1 \text{ MeV}) \tag{D-5}$$

or, solving for the flux

$$\phi(E > 1 \text{ MeV}) = \frac{D_i}{K_i P_i \bar{\sigma}_n} . \tag{D-6}$$

D-3

The revised method essentially uses this last equation to calculate the capsule flux from the measured activities D_i and the average cross section, $\bar{\sigma}_n$, calculated from previous analyses (see Table D-1). Note that $\bar{\sigma}_n$ is dependent upon the capsule azimuthal location since the calculated flux spectrum used to obtain $\bar{\sigma}_n$ differs from the 11- and 26-degree locations due to differences in distances from the core.

The measured activity (at least for the ^{137}Cs activity) is representative of irradiations in all cycles previous to the measurement. For the AN1-A capsule, this includes irradiation in cycle 1A of ANO-1 and cycles 1, 2, and 3 of Davis-Besse. The irradiation history of the capsule is represented by the P_i term which accounts for production and decay of the product isotope by cycle as a function of time at a particular power level. By accounting for production and decay during previous irradiation cycles and the use of an appropriate P_i, the flux for the last cycle, or cycles, can be determined. Previous capsule analyses have determined cycle-by-cycle capsule activities and fast fluxes for cycle 1A of ANO-1 and cycles 1 and 2 of Davis-Besse for symmetric capsule locations. Thus, the cycle 3 activity can be determined from

$$A_3 = A_T - \sum_i A_i e^{-\lambda t_i} \qquad (D-7)$$

where A_3 = cycle 3 activity,

A_T = the measured activity at the end of cycle 3 (EOC 3),

t_i = decay period from EOC_i to EOC 3.

Using P_i for cycle 3, the cycle 3 capsule fluxes can be determined. By appropriate modification of A_i and P_i, capsule fluences for any combination of cycles can be determined. For capsule AN1-A, capsule fluxes for cycle 3, 2 and 3, and 1, 2, and 3 were determined (see Table 6-4).

Capsule fluence is obtained from the product of capsule flux and irradiation time period. For this analysis, integrated capsule fluences were obtained from the sum of fluences for the Davis-Besse and the ANO-1 irradiations. Three such values were obtained, i.e., from the three methods of calculating Davis-Besse fluxes (see Table 6-4). The reported capsule fluence represented the average of these values. This was done to reduce

Babcock & Wilcox
a McDermott company

dependence on any particular cycle measurement to mitigate effects due to errors associated with that cycle's measurement.

1.2. Vessel Flux and Fluence

The vessel flux calculation essentially uses the same method as previous analyses. Energy-dependent neutron fluxes at the reactor vessel were determined by a discrete ordinates solution of the Boltzmann transport equation with the two-dimensional code DOT4. The ANO-1 reactor was modeled from the core out to the primary concrete shield in R-θ geometry (based on a plan view along the core midplane and one-eighth core symmetry in the azimuthal dimension). The reactor model contained the following regions: core, liner, bypass coolant, core barrel, inlet coolant, thermal shield, inlet coolant (downcomer), pressure vessel, cavity, and concrete shield. Input data to the code included a PDQ calculated pin-by-pin, time-averaged power distribution, CASK 23E 22-group microscopic neutron cross sections,[8] S_8 order of angular quadrature, and P_3 expansion of the scattering cross section matrix. Reactor conditions, i.e., power distribution, temperature and pressure, were averaged over the irradiation period. Because of computer storage limitations, it was necessary to use two geometric models to cover the distance from core to primary shield. A boundary source output from Model A (core to downcomer region) was used as input to Model B (thermal shield to primary shield). In this way, the effect of the specific power distribution of ANO-1 cycle 5 on vessel fluence was included in the calculation.

Flux output from the DOT4 calculations required only an axial distribution correction to provide absolute values. An axial shape factor (local to average axial flux ratio) was obtained from predicted fuel burnup distributions in the peripheral fuel assemblies nearest the vessel, i.e., the core flats region. This procedure assumes that the axial fast flux shape at the core edge and the pressure vessel are equivalent. In the 177-FA reactor geometry, this is considered to be a conservative assumption because axial shape should tend to flatten as distance from the core increases. An axial factor of 1.15 was applied to the calculated flux for the ANO-1 reactor vessel. This axial factor was time-averaged over the irradiation period.

D-5

In addition to the axial shape factor, one other factor is applied to the flux to normalize it to measured values. From previous analyses, using equivalent DOT4 models and constant terms in equation D-2 to obtain the calculated activity, a normalization factor of about 0.95 has been consistently obtained. Although this factor is strictly correct only at the capsule location, it is assumed to be applicable to all locations in the reactor model. This assumption is based on the following considerations: (1) B&W 177-FA reactors have essentially the same configuration and (2) the pressure vessel and capsule are separated by only 15 cm of water so that it is unlikely that any significant change in accuracy would occur in this distance. Due to the consistency of this factor at the capsule and the considerations above, it will be applied to the ANO-1 cycle 5 calculated vessel flux with only a minor correction to account for DOT4 model change and revised ^{137}Cs yield values which have been implemented since the previous analyses. The model change incorporated a more accurate water temperature in the core former region. The previous model assumed that this water region was at the average core water temperature; recent information indicates that an average of the core and downcomer temperature is more realistic. This decrease in water temperature increases its density. From DOT4 studies, this density increase causes a reduction in the vessel flux by approximately 4%. The second correction is due to use of recently recommended ASTM ^{137}Cs yield values from the fission of ^{238}U and ^{237}Np. Use of the recommended values reduce the calculated activity used to obtain the normalization factor by approximately 5%. Since both changes reduce the calculated activity, i.e., the denominator in equation D-2, the 0.95 normalization factor must be increased. Thus, the effective normalization factor becomes

$$1.04 \times 1.05 \times 0.95 = 1.04.$$

This normalization factor was applied to the calculated fluxes for this analysis.

2. Vessel Fluence Extrapolation

For up-to-date operation, fluence values in the reactor vessel are calculated as described above. Extrapolation to future operation is required for the prediction of vessel life based on minimum USE and for the calculation of pressure-temperature operation curves. Three time periods are

D-6

considered: (1) to-date operation for which vessel fluence has been calcu-
lated, (2) designed future fuel cycles for which PDQ calculations have been
performed for fuel management analysis of reload cores, and (3) future fuel
cycles for which no analyses exist. Data from time period 1 are extrapo-
lated through time period 2 based on the premise that excore flux is propor-
tional to the fast flux that escapes the core boundary. Thus, for the ves-
sel,

$$\phi_{v,C} = \frac{\phi_{e,C}}{\phi_{e,R}} \times \phi_{v,R}$$

where the subscripts are defined as v = vessel, e = core escape, R = refer-
ence cycle, C = a future fuel cycle.

Core escape flux is available from PDQ output. Extrapolation from time pe-
riod 2 through time period 3 is based on the last designed fuel cycle in
period 2 having the same relative power distribution as an "equilibrium"
fuel cycle. Generally, the designed fuel cycles include several cycles
into the future, 6 and 7 for ANO-1. Therefore, the last cycle in time
period 2 should be representative of an "equilibrium" cycle. Data for
ANO-1 are listed in Table D-2.

This procedure is considered preferable to the alternative of assuming that
lifetime fluence is based on a single, hypothetical "equilibrium" fuel
cycle because this procedure accounts for all known power distributions.
In addition, errors that may result from the selection of a hypothetical
"equilibrium" cycle are reduced.

Table D-1. Spectrum-Averaged Cross Sections

Reaction	Average cross section, $\bar{\sigma}_n$ (barns)
$^{58}Ni(n,f)^{58}Co$	0.1222
$^{54}Fe(n,f)^{54}Mn$	0.09283
$^{238}U(n,f)^{137}Cs$	2.416
$^{237}Np(n,f)^{137}Cs$	0.4037

Table D-2. Extrapolation of Reactor Vessel Fluence

Cycle	Core escape flux, n/cm^2-s	Time, EFPY	Cumulative time, EFPY	Vessel flux, n/cm^2-s	Vessel fluence, n/cm^2	
					Time interval	Cumulative
1A	0.482(+14)	0.95	0.95	1.39(+10)	4.17(+17)	4.17(+17)
1B-4	0.509(+14)	2.88	3.83	1.46(+10)	1.32(+18)	1.73(+18)
5	0.406(+14)	1.22	4.10	1.03(+10)	3.96(+17)	2.13(+18)
6	0.408(+14)	1.10	5.20	1.04(+10)[a]	3.59(+17)	2.49(+18)
7	0.397(+10)	1.15	6.35	1.01(+10)[a]	3.67(+17)	2.86(+18)
>7	0.397(+10)[b]	1.65	8.0	1.01(+10)[a]	5.26(+17)	3.38(+18)
>7	0.397(+10)[b]	7.0	15.0	1.01(+10)[a]	2.23(+18)	5.61(+18)
>7	0.397(+10)[b]	17.0	32.0	1.01(+10)[a]	5.42(+18)	1.10(+19)

[a]Predicted value based on proportionality of core escape flux.

[b]After cycle 7, core escape flux is expected to be that of cycle 7, i.e., cycle 7 is "equilibrium" cycle.

APPENDIX E
Capsule Dosimetry Data

Babcock & Wilcox
a McDermott company

Table E-1 lists the composition of the threshold detectors and the equivalent cadmium thickness used to reduce competing thermal reactions. Table E-2 shows capsule AN1-A measured activity per gram of target material (i.e., per gram of uranium, nickel, etc.). Activation cross sections for the various materials were flux-weighted with a ^{235}U fission spectrum (Table E-3).

Table E-1. Detector Composition and Shielding

Monitors	Shielding	Reaction
10.38% U-Al	Cd-Ag 0.03" Cd	$^{238}U(n,f)$
1.44% Np-Al	Cd-Ag 0.03" Cd	$^{237}Np(n,f)$
Ni 100%	Cd-Ag 0.03" Cd	$^{58}Ni(n,p)^{58}Co$
0.66 wt % Co-Al	Cd-Ag 0.03" Cd	$^{59}Co(n,\gamma)^{60}Co$
0.66 wt % Co-Al	None	$^{59}Co(n,\gamma)^{60}Co$
Fe 100%	None	$^{54}Fe(n,p)^{54}Mn$

Babcock & Wilcox
a McDermott company

Table E-2. Capsule AN1-A Dosimeter Activities

Dosimeter material	Dosimeter reaction	Dosimeter activity, μCi/gm of target			
		AD1	AD2	AD3	AD4
Ni	$^{58}Ni(n,p)^{58}Co$	2990	2508	2429	3778
Fe	$^{54}Fe(n,p)^{54}Mn$	1805	1484	1398	2201
^{238}U-Al	$^{238}U(n,f)^{137}Cs$	13.4	11.19	9.68	15.04
^{237}Np-Al	$^{237}Np(n,f)^{137}Cs$	78.54	64.64	53.54	89.81

Table E-3. Dosimeter Activation Cross Sections, b/atom[a]

G	Energy range, MeV	$^{237}Np(n,f)$	$^{238}U(n,f)$	$^{58}Ni(n,p)$	$^{54}Fe(n,p)$
1	12.2 - 15	2.323	1.050	4.830(-1)	4.133(-1)
2	10.0 - 12.2	2.341	9.851(-1)	5.735(-1)	4.728(-1)
3	8.18 - 10.0	2.309	9.935(-1)	5.981(-1)	4.772(-1)
4	6.36 - 8.18	2.093	9.110(-1)	5.921(-1)	4.714(-1)
5	4.96 - 6.36	1.541	5.777(-1)	5.223(-1)	4.321(-1)
6	4.06 - 4.96	1.532	5.454(-1)	4.146(-1)	3.275(-1)
7	3.01 - 4.06	1.614	5.340(-1)	2.701(-1)	2.193(-1)
8	2.46 - 3.01	1.689	5.272(-1)	1.445(-1)	1.080(-1)
9	2.35 - 2.46	1.695	5.298(-1)	9.154(-2)	5.613(-2)
10	1.83 - 2.35	1.677	5.313(-1)	4.856(-2)	2.940(-2)
11	1.11 - 1.83	1.596	2.608(-1)	1.180(-2)	2.948(-3)
12	0.55 - 1.11	1.241	9.845(-3)	6.770(-4)	6.999(-5)
13	0.111 - 0.55	2.34(-1)	2.432(-4)	1.174(-6)	1.578(-8)
14	0.0033-0.111	6.928(-3)	3.616(-5)	1.023(-7)	1.389(-9)

[a]ENDF/B5 values have been flux-weighted (over CASK energy groups) based on a ^{235}U fission spectrum in the fast energy range plus a 1/E shape in the intermediate energy range.

Babcock & Wilcox
a McDermott company

APPENDIX F
References

Babcock & Wilcox
a McDermott company

[1] A. L. Lowe, Jr., _et al._, Analysis of Capsule AN1-E From Arkansas Power & Light Company, Arkansas Nuclear One -- Unit 1, Reactor Vessel Material Surveillance Program, BAW-1440, Babcock & Wilcox, Lynchburg, Virginia, April 1977.

[2] A. L. Lowe, Jr., _et al._, Analysis of Capsule AN1-B From Arkansas Power & Light Company's Arkansas Nuclear One, Unit 1, Reactor Vessel Materials Surveillance Program, BAW-1698, Babcock & Wilcox, Lynchburg, Virginia, November 1981.

[3] G. J. Snyder and G. S. Carter, Reactor Vessel Material Surveillance Program, BAW-10006A, Rev. 3, Babcock & Wilcox, Lynchburg, Virginia, January 1975.

[4] A. L. Lowe, Jr., K. E. Moore, and J. D. Aadland, Integrated Reactor Vessel Material Surveillance Program, BAW-1543, Rev. 2, Babcock & Wilcox, Lynchburg, Virginia, February 1984.

[5] A. L. Lowe, Jr., _et al._, Analyses of Capsule RS1-D, Sacramento Municipal Utility District, Rancho Seco Unit 1, Reactor Vessel Material Surveillance Program, BAW-1792, Babcock & Wilcox, Lynchburg, Virginia, October 1983.

[6] H. S. Palme and H. W. Behnke, Methods of Compliance With Fracture Toughness and Operational Requirements of Appendix G to 10 CFR 50, BAW-10046A, Rev. 1, Babcock & Wilcox, Lynchburg, Virginia, July 1977.

[7] DOT4 -- Two-Dimensional Discrete Ordinates Radiation Transport Code, NPGD-TM-559, Rev. 2, Babcock & Wilcox, Lynchburg, Virginia, August 1981.

[8] CASK -- 40-Group Coupled Neutron and Gamma-Ray Cross Section Data, RSIC-DLC-23E, Radiation Shielding Information Center, March 1975.

Babcock & Wilcox
a McDermott company